Submitted to Physical Review

UCRL-19014
Preprint



# SELF-INDUCED TRANSPARENCY

S. L. McCall and E. L. Hahn

May 1969

AEC Contract No. W-7405-eng-48



LAWRENCE RADIATION LABORATORY
UNIVERSITY of CALIFORNIA BERKELEY

UCRL-19014

## DISCLAIMER

# SELF-INDUCED TRANSPARENCY*

S. L. McCall† and E. L. Hahn

Inorganic Materials Research Division, Lawrence Radiation Laboratory,
and Department of Physics,
University of California, Berkeley, California

## ABSTRACT

Above a critical power threshold for a given pulse width a short pulse of coherent traveling wave optical radiation is observed to propagate with anomalously low energy loss while at resonance with a two quantum level system of absorbers. The line shape of the resonant system is determined by inhomogeneous broadening, and the pulse width is short compared to dissipative relaxation times. A new mechanism of self-induced transparency, which accounts for the low energy loss, is analyzed in the ideal limit of a plane wave which excites a resonant medium with no damping present. The stable condition of transparency results after the traversal of the pulse through a few classical absorption lengths into the medium. This is signified after the initial pulse evolves into a symmetric hyperbolic secant pulse function of time and distance, and has a specific area as a "$2\pi$ pulse." Ideal transparency then persists when coherent induced absorption of pulse energy during the first half of the pulse is followed by coherent induced emission of the same amount of energy back into the beam direction during the second half of the pulse. The effects of dissipative relaxation times upon pulse energy, pulse area, and pulse delay time are analyzed to first order in the ratio of short pulse width to long damping time. Analysis

---

* Supported by the National Science Foundation

† Present address: Bell Telephone Laboratories, Murray Hill, N.J.

shows that the $2\pi$ pulse condition can be maintained if losses caused by damping are compensated by beam focusing. In an amplifying inhomogeneously broadened medium an analytic "$\pi$ pulse area" solution is presented in the limit of a sharp rising pulse leading edge. The dynamics of self-induced transparency are studied for the particular effects of Doppler velocities upon a resonant gas. The analysis of transparency for random orientations of dipole moments associated with degenerate rotational states yields modified forms of self-induced transparency behavior which indicates finite pulse energy loss in some cases as a function of distance. The effect of self-induced transparency on the photon echo is considered. Experimental observations of self-induced transparency are made in a ruby sample at resonance with a pulsed ruby laser beam. Single and multiple $2\pi$ pulse outputs are observed, and pulse areas are measured in the range of $2\pi$. The experimental results are compared with the predictions of the ideal plane wave theory. Deviations from the ideal plane wave theory are discussed. An analysis is made of the effect of a transverse mode of the propagating beam upon the transparency properties of the pulse.

# I. INTRODUCTION

The development of sources of pulsed coherent radiation has initiated investigations of the behaviour of coherent traveling waves as they interact with media which have absorption bands near or at the frequency of the applied pulse. Of particular interest are resonant absorbing media characterized by localized two level transitions which are excited by optical[1] and phonon[2] radiation. The absorption of low intensity coherent or incoherent radiation can usually be interpreted in terms of linear dispersion theory, particularly if the ground state energy levels of the absorbing medium (or excited states in the case of a prepumped active amplifying medium) are only slightly depopulated by the radiation. As the resonant traveling wave radiation intensity is increased, the linear problem[3] can be perturbed to account for the onset of weak nonlinearities[4]. If damping is not too severe, transient oscillations in state populations can exist during and after the application of pulsed radiation[5]. The transient behaviour of two level systems interacting with standing waves[6] in cavities is closely related to fundamental aspects of pulsed traveling wave resonance phenomena. For very large intensities of pulsed coherent radiation encompassed by optical, phonon, and microwave radiation, the pulse width times have a critical effect if they are comparable to or shorter than the dissipative damping times of the resonant medium. The state population changes become markedly nonlinear and time dependent: the resonance susceptibility of the medium is then a strong function of the driving field.

Usual perturbation treatments of strongly driven resonance phenomena cannot tractably reveal many rather surprising nonlinear propagation

effects. The mere application of simple rate equations to describe the population of quantum states is invalid, and the use of standard absorption and emission coefficients to examine the pulsed response of systems at resonance in the usual manner can be inadequate or incorrect. The time dependence of the off-diagonal elements that represent the induced polarization plays a principle role in the description of coherent superpositions of quantum levels. The simplest two level system is one where each level is non-degenerate, and it is this case which will be the main one to be discussed here. We will speak in terms of optical states and electric dipole moments, but our analysis will also apply to cases where magnetic or quadrupole moments are involved in the resonance process. The pulsed radiation can involve magnetic, electric, magnon, phonon, or other classically describable fields.

A striking manifestation of the nonlinear resonance response to pulses of coherent light is the photon echo effect[7]. This phenomenon, the optical analogue of the spin echo effect[8], illustrates the collective superradiant state described by Dicke[6], which radiates energy coherently into the electromagnetic field. In the case of spin systems, the same effect is spoken of in terms of free precession coherence, where spin ensembles radiate coherently into a resonant cavity. In this work we consider the interaction of a light pulse with a medium which has dimensions large compared to a wave length, and is not contained in a cavity. The medium dimensions may or may not be large in comparison with the linear absorption length. The optical resonators are assumed to be distributed over a spectrum of frequencies determined by an internal spread of fixed two level splittings. This spread defines the line shape as inhomogeneously broadened. If a weak pulse enters the medium, a fraction

of the pulse energy is absorbed and retained as excitation energy of the two level system in the beginning length of the sample, and after a few absorption lengths the pulse intensity has disappeared according to the usual Beer's law[9] of absorption. Although the dipoles are left excited after the pulse has gone by, they cannot reradiate power because they quickly dephase among themselves, owing to the broad pulse spectrum over which they have been excited. While a given group of dipoles is excited coherently by the pulse, absorption is induced because of the familiar resonance property that the driving electric field is opposed by an electric field radiated by the dipoles. However, if the initial pulse power is sufficient to excite resonant dipoles into a predominately inverted or "pumped" state before the pulse has subsided, some energy of induced emission radiation will be returned coherently into the remaining portion of the pulse. The electric field radiated by the induced polarization will then add to the driving field. Once this emission process takes hold to the slightest degree, it becomes favored more and more as the pulse propagates into the medium until the following equilibrium condition is reached. The energy of induced emission, transferred to the light beam during the last half of the pulse, becomes equal to the energy of induced absorption transferred from the light beam, during the first half of the light pulse. This constitutes the dynamic condition of self-induced transparency[10], and the final pulse is characterized as a "$2\pi$ pulse" in the same way a gyromagnetic spin system can be excited to upper states and returned to the ground state by a pulse of radiofrequency power. Attenuation caused by damping of the resonant dipoles or by background scattering losses is assumed to be absent or small, but the transparency effect retains its

essential description in the presence of real damping if the initially applied pulse has a width short compared to, or even comparable with the damping time. In the simple case of a plane wave the injected pulse evolves to a final symmetric shape which is a $2\pi$ hyperbolic secant function (hereafter denoted as $2\pi$ h.s.) of time and distance. The pulse velocity becomes less than that of non-resonant light in the medium because of the continual absorption of energy from the pulse leading edge and emission of energy into the pulse trailing edge. When the pulse velocity is considerably less than the light velocity, the pulse energy is described as belonging predominantly to the resonant medium rather than to the electromagnetic field.

The transparency effect is not necessarily restricted to the special case of single pulse transmission. For example, in an extended medium the effect is an aid in predicting some properties of the photon echo which evolves as a third pulse following the application of two previous pulses. In another situation a light wave of sufficient intensity which is turned on and left on will sharpen in its leading edge as it travels through the medium. Field oscillations will finally develop following the leading edge which will decay in a damping time determined by losses in the medium. Where the damping is small, a single pulse of large area may split up into two or more self propagating individual $2\pi$ h.s. pulses which have widths less than the damping time of the medium. Generally, the final pulse may be characterized as a superposition of $2\pi$ h.s. pulses of various widths, phases, delay times, and center frequencies.

Initial computer calculations[11] indicated specific rules for the propagating pulse area as a function of distance. These rules implied the existence of small pulse energy loss during pulse propagation, which

led to an analytic investigation of the resultant pulse shape. According to the assumptions of the ideal plane wave model, the pulse shape evolves to a $2\pi$ h.s. form for which the losses are not merely small, but precisely zero. The transparency effect was demonstrated[10] experimentally in the case of ruby laser pulsed light acting on a passive ruby sample tuned to the driving pulse. Subsequently the transparency effect was demonstrated in a gas[12] by Slusher and Patel in the case of 10.6 micron radiation pulses from a $CO_2$ laser passing through a gaseous medium of resonant $SF_6$.

In view of the rapid development of "Q-switch"[1] and mode-lock[13] pulse techniques which produce laser pulses in the range of $10^{-8}$ to $10^{-12}$ seconds, such pulses should propagate over anomalously large distances through real systems with electron dipole damping times in this range. The onset of attenuation effects are themselves of critical interest in the measurement of short lifetimes in resonant atomic states, electron band states in solids, and collision damping times and cross sections in gases. The shape and area of the self propagating pulses are themselves a measure of transition dipole moments, relaxation times, and a number of other properties ultimately connected with the nature of the medium line shape and resonance structure. The analysis in this paper applies as well to many situations where the medium is prepared initially in pumped excited states. This is a condition common to all lasers and amplifying media, and the transparency effect appears to be an important consideration for analyzing the nonlinear character of laser pulse steepening, amplification, and final output pulse character.

The analysis of the simple case of a two level system interacting with circularly polarized light is initially presented in this paper. This case is chosen because of the close physical correspondence of its

vector model to macroscopic physical quantities, so that we may utilize easily the concepts of nuclear magnetic resonance. Some of the resultant restrictions are subsequently removed in order to discuss other related cases.

## II. ANALYSIS OF SELF-INDUCED TRANSPARENCY

### Assumptions

The several analytic results which describe the optical self-induced transparency effect can be derived on the basis of a semi-classical description which involves a number of assumptions. For simplicity consider a circularly polarized traveling plane wave light pulse of optical frequency $\omega$, given by

$$\underset{\sim}{E}(z,t) = \mathcal{E}(z,t)[\hat{i}\cos(\omega t - kz - \phi(z)) + \hat{j}\sin(\omega t - kz - \phi(z))], \qquad (1)$$

which enters and traverses a medium in the direction $\hat{k}$ of increasing distance z, where the orthogonal unit vectors $\hat{i}$ and $\hat{j}$ are transverse to the propagation direction. The strength of the electric field modulus $\mathcal{E}$ is sufficiently large that the electromagnetic field may be regarded as classical; and yet it is small enough so that $|p\mathcal{E}| \ll \hbar\omega$, where p is the interacting dipole moment. We may consistently assume that

$$\left|\frac{\partial \mathcal{E}}{\partial z}\right| \ll \left|\frac{\mathcal{E}}{\lambda}\right| \text{ and } \left|\frac{\partial \mathcal{E}}{\partial t}\right| \ll \omega|\mathcal{E}|, \qquad (2)$$

where $k = \eta\frac{\omega}{c} = \frac{2\pi\eta}{\lambda}$, $\lambda$ is the free space wave length, $\eta$ is the host refractive index, c the speed of light in vacuum, and $\phi$ is an arbitrary phase angle not dependent on the time t. Eqs. (1) and (2) imply the neglect of coherent back scattering. Only coherent forward scattering

applies in the regime $\alpha^{-1} \gg \lambda$, where $\alpha^{-1}$ is the optical absorption length attributed to the absorbing dipoles which respond at frequency $\omega$ of weak monochromatic light. The refractive index $\eta$ is assumed to be unaffected by the light pulse intensity, and we therefore neglect effects which may arise from nonlinear generation of light with frequencies not close to $\omega$. Frequency modulation and pulling effects are not considered by assuming that there is no time dependence of $\phi$. This restriction is consistent with all of the assumptions made here.

The medium contains N particles per $cm^3$ initially in the ground state of two energy eigenstates between which electric dipole transitions can occur. The induced electric dipole polarization can be accurately represented as a continuum (see Appendix A); and the resultant optical resonance line is inhomogeneously broadened. In solids such a broadening could be caused by a distribution of static crystalline electric and magnetic fields, and in optically resonant gases the distribution of Doppler frequencies serves as the inhomogeneous broadening mechanism. The effect of other linewidth contributions is neglected, such as lifetime or collision broadening caused by phonon interactions or by any other homogeneous contribution to the linewidth. The resultant distribution of natural frequencies $\omega_o$ of a given ion, atom, or molecule (hereafter designated as a "dipole") is described by the symmetrical spectral density function $g(\Delta\omega)$, where $\int_{-\infty}^{\infty} g(\Delta\omega)d(\Delta\omega) = 1$ and $\Delta\omega = \omega_o - \omega$. The applied frequency $\omega$ is tuned to the center of the spectral function $g(\Delta\omega)$. The dipoles are coupled only by their interaction with the plane wave electromagnetic field, and the direct dipole-dipole coupling is assumed to be negligibly small.

Resonance Dynamics of a Two Level System

At the entry face z = 0 of the medium, let $\phi(0) = 0$, and define $\mathcal{E}(0,t)$ in Eq. (1) as an arbitrary input pulse envelope shape, perhaps generated by a laser source. In the medium the interaction Hamiltonian of the two level system with no damping terms included is expressed as

$$\mathcal{H} = \mathcal{H}_o - \underset{\sim}{p_o} \cdot \underset{\sim}{E}(z,t), \tag{3}$$

where $\mathcal{H}_o$ is the main interaction, internal to the two level system, which determines the splitting $\hbar\omega_o$. The electric dipole moment operator is defined as

$$\underset{\sim}{p_o} = p(\hat{i}\sigma_x + \hat{j}\sigma_y), \tag{4}$$

where $p = p_x = p_y$ are magnitudes of the respective components of electric dipole moments[14]. The Pauli operator $\underset{\sim}{\sigma}$ has transformation properties identical to the spin operator $\underset{\sim}{I}$ which occurs in magnetic resonance problems, where $\frac{1}{3}\underset{\sim}{\sigma} \cdot \underset{\sim}{\sigma}$ is the identity matrix. With the definitions that

$$\underset{-}{p_+} = p(\sigma_x \pm i\sigma_y),$$

$$\underset{-}{E_+}(z,t) = \mathcal{E}(z,t)e^{+i[\omega t - kz - \phi(z)]} \tag{5}$$

Eq. (3) becomes

$$\mathcal{H} = \mathcal{H}_o - \tfrac{1}{2}[p_+E_-(z,t) + p_-E_+(z,t)]. \tag{6}$$

The two quantum level solutions for the expectation value of the source electric dipole moment per $cm^3$ have been shown[15] to be of the same form as those obtained for the magnetic moment in nuclear induction[16]. We review briefly a popular density matrix method which provides a concise method to obtain macroscopic equations of motion of the dipole system, needed in our analysis. The reader informed on this point may skip this review and proceed with the analysis immediately following Eq. (17). The density matrix method may ultimately embrace treatment of relaxation damping, or of cases where an arbitrary mixture of $\sigma_{\pm}$ and $\pi$ optical polarizations may occur, which indicate respectively polarizations transverse and parallel to a defined axis in the medium.

Considering only its time dependence, let the dipole two-level wave function be given by

$$\psi = a_1(t)\psi_1 + a_2(t)\psi_2, \tag{7}$$

with population coefficients $a_1(t)$, $a_2(t)$ and stats functions $\psi_1, \psi_2$ assigned respectively to excited (1) and ground (2) states. The dependence of $\psi$ upon z and the phase of traveling wave excitation must eventually be included. In our particular experiment the ground state is completely populated before dipole transitions are induced, and therefore $|a_2(0)|^2 = 1$, $|a_1(0)|^2 = 0$ at time $t = -\infty$. The initial density matrix is given by

$$\rho(0) \equiv \begin{pmatrix} 0 & 0 \\ 0 & 1 \end{pmatrix}. \tag{8}$$

The operators in Eqs. (5) and (6) are expressed in matrix form as

$$p_+ = p\sigma_+ \equiv 2p \begin{pmatrix} 0 & 1 \\ 0 & 0 \end{pmatrix},$$

$$p_- = p\sigma_- \equiv 2p \begin{pmatrix} 0 & 0 \\ 1 & 0 \end{pmatrix}, \text{ and}$$

$$\mathcal{H}_o = \frac{\hbar\omega_o}{2} \begin{pmatrix} 1 & 0 \\ 0 & -1 \end{pmatrix}. \tag{9}$$

The time dependent equation

$$i\hbar\dot{\rho}(t) = [\mathcal{H},\rho(t)] \tag{10}$$

for the density matrix is conveniently examined in a representation in which $\mathcal{H}$ and $\rho(t)$ transform as follows:

$$\mathcal{H}^* = T\mathcal{H}T^{-1} - \frac{\hbar\omega}{2}\sigma_z = \frac{\hbar\Delta\omega}{2}\sigma_z - \frac{\hbar\kappa c}{2}\sigma_x \tag{11}$$

$$\rho^*(t) = T\rho(t)T^{-1}; \tag{12}$$

where $T = e^{i(\sigma_z/2)[(\omega t - kz - \phi(z)]}$, $\kappa = \frac{2p}{\hbar}$, and $\Delta\omega = \omega_o - \omega$.

In developing the time dependent behaviour of $\rho$ it is understood that $\rho \equiv \rho(t,\Delta\omega,z)$, although the notation is restricted to writing $\rho = \rho(t)$. In the case of the simple $\mathcal{H}_o$ matrix given in Eq. (9), the T transformation allows one to view $\mathcal{H}_o$ as the interaction Hamiltonian in a frame of reference rotating about the laboratory z axis at frequency $\omega$. Eq. (10) therefore transforms to

$$i\hbar\dot{\rho}^*(t) = [\mathcal{H}^*,\rho^*(t)]. \tag{13}$$

In this representation the time derivative of the expectation value of any operator $F^*$ is

$$\frac{d\langle F^*(t)\rangle}{dt} = \frac{i}{\hbar}\mathrm{Tr}[F^*(t)[\mathcal{H}^*, F^*]]. \tag{14}$$

The operators $F^*$ of interest here are given by $\sigma_z, \sigma_x$, and $\sigma_y$, where the spectral energy density is defined as

$$W = \frac{N\hbar\omega_o}{2}\langle\sigma_z\rangle, \tag{15}$$

and the transverse electric polarization density is

$$u+iv = \frac{Np}{2}\langle\sigma_x+i\sigma_y\rangle. \tag{16}$$

The terms u and v can be identified as the electric dipole dispersion and absorption components respectively, in accord with the undamped Bloch equation notation[16]. These components combine with a pseudo polarization $-\frac{\kappa W}{\omega}$, which plays the role of transverse magnetization $M_z$ in the original Bloch notation, to define a vector polarization $P_z$. A real electric polarization $P_z$ may in fact exist, but would not be involved in our treatment here. The three components together define a fictitious vector polarization

$$\underset{\sim}{P} = \hat{u}_o\, u + \hat{v}_o - \hat{w}_o \frac{W\kappa}{\omega} \tag{17}$$

in the frame of reference rotating at frequency $\omega$ about unit vector $\hat{w}_o$, defined in this case along the laboratory z axis parallel to the direction of light propagation. The unit vectors

$\hat{u}_o, \hat{v}_o, \hat{w}_o$ form a mutually orthogonal set. From Eqs. (14), (15), and (16) the time dependence of $\underset{\sim}{P}$ above is obtained in a form of the familiar torque equation

$$\frac{d\underset{\sim}{P}}{dt} = \underset{\sim}{P} \times [\hat{u}_o \kappa \mathcal{E}(z,t) + \hat{w}_o \Delta\omega]. \tag{18}$$

Coupling to Maxwell's Equations

The final step before presenting an analysis of the pulse propagation is to couple Eq. (18) to Maxwell's equations for propagation of a circularly polarized plane wave. From Eq. (5) let the traveling wave

$$E_+(z,t) = \mathcal{E}(z,t) e^{i[\omega t - kz + \phi(z)]}, \tag{19}$$

with parameters defined in Eq. (1), be the complex solution of the wave equation

$$\frac{\partial^2 E_+(z,t)}{\partial z^2} = \frac{\eta^2}{c^2} \frac{\partial^2 E_+(z,t)}{\partial t^2} + \frac{4\pi}{c^2} \frac{\partial^2 P_+(z,t)}{\partial t^2}. \tag{20}$$

net resonant

The ~~resonance induced net~~ complex polarization $P_+(z,t)$ is given by

$$P_+(z,t) = \int_{-\infty}^{\infty} g(\Delta\omega)[u(\Delta\omega,z,t) + iv(\Delta\omega,z,t)] e^{i[\omega t - kz - \phi(z)]} d(\Delta\omega). \tag{21}$$

Any symmetric distribution function $g(\Delta\omega)$ centered about the applied frequency $\omega$ is acceptable; and in the particular case where $g(\Delta\omega)$ is a bell shaped function, $(1/T_2^*)\sec^{-1}$ is proportional to $g(0)^{-1}$, and is an approximate measure of the

line width. The assumed relations of Eq. (2), which state that $\mathcal{E}(z,t)$ is slowly varying, also assures a similar behaviour for $P_+(z,t)$ After substituting Eqs. (19) and (21) into Eq. (20), the relations of Eq. (2) permit slowly varying terms to be dropped, and the following equations result:

$$\frac{\partial \mathcal{E}}{\partial z} = -(\eta/c)\frac{\partial \mathcal{E}}{\partial t} - \frac{2\pi\omega}{\eta c}\int_{-\infty}^{\infty} v(\Delta\omega,z,t)g(\Delta\omega)d(\Delta\omega); \tag{22}$$

$$\kappa\,\frac{\partial \phi(z)}{\partial z}\,\mathcal{E} = \frac{2\pi\omega^2}{c^2}\int_{-\infty}^{\infty} u(\Delta\omega,z,t)g(\Delta\omega)d(\Delta\omega). \tag{23}$$

To complete the array of required scalar equations, Eq. (18) is re-written as follows, but with the addition of phenomenological damping terms according to the Bloch notation[16]:

$$\frac{du}{dt} = v\Delta\omega - u/T_2', \tag{24}$$

$$\frac{dv}{dt} = -u\Delta\omega - \frac{\kappa^2}{\omega}\mathcal{E}W - v/T_2', \tag{25}$$

$$\frac{dW}{dt} = v\mathcal{E}\omega - \frac{(W-W_o)}{T_1}. \tag{26}$$

Any incoherent damping effects, such as spontaneous emission or life-time broadening mechanisms associated with collisions, are included in the relaxation time $T_2'$. The time $T_1$ defines the energy damping time constant associated with relaxation which restores the energy of the optical system to the ground state value $W_o = -N\left(\frac{\hbar\omega}{2}\right)$. The total optical linewidth is defined approximately as

$$\frac{1}{T_2} \sim \frac{1}{T_2'} + \frac{1}{T_2^*}. \tag{27}$$

In turn, $\frac{1}{T_2'} \sim \frac{1}{T_1} + \frac{1}{T_2''}$, where $T_2''$ pertains to any lifetime broadening mechanism which does not significantly alter the population distribution between the two levels of the system connected with the resonance. Instead $T_2''$ accounts for the broadening of either or both levels by relaxation processes that do not cause transitions between the two levels. Such broadening is produced, for example, by electric Stark or magnetic Zeeman frequency modulation of the level eigenvalues because of incoherent local field fluctuations, or because of very rapid relaxation from one or both of the two levels to a third level which is not directly involved in the externally excited resonance. A rigorous treatment of damping is of course not intended in specifying the above relaxation times; these phenomenologically represent the kind of damping which may occur. For the limit of ideal self-induced transparency of electric field pulses of width $\tau$, the inequalities $\tau \ll T_2'$ and $\tau \gg \omega^{-1}$ are to apply in the analysis to follow.

The Area Theorem and Its Properties

For those oscillators exactly at resonance in the absence of relaxation, let $\Delta\omega=0$, and define $T_1 = T_2' = \infty$ in Eqs. (24), (25) and (26) for all $\Delta\omega$. Therefore

$$v(0,z,t) = N\sin\varphi(z,t), \tag{28}$$

$$W(0,z,t) = W_o\cos\varphi(z,t), \tag{29}$$

where $$\varphi(z,t) = \kappa\int_{-\infty}^{t} \mathcal{E}(z,t')dt' \tag{30}$$

expresses the angle through which the fictitious polarization vector $\underset{\sim}{P}$ at exact resonance ($\Delta\omega=0$) is turned at time t by the $\mathcal{E}$ field pulse. The angle $\varphi$ therefore expresses the area of the pulse developed up to time t. Let the area A of the entire pulse be defined when the upper limit $t \to \infty$ applies in Eq. (30). Therefore, $A = \kappa\int_{-\infty}^{\infty}\mathcal{E}(z,t')dt'$. The total tipping angle of $\underset{\sim}{P}(0,z,\infty)$ is $\theta=\tan^{-1}\left\{\frac{\omega v(0,z,\infty)}{\kappa W(0,z,\infty)}\right\}$ which may not be numerically equal to A in other physical situations.

We now can show how the behaviour of the component $v(0,z,t)$ at exact resonance is connected with the motion of components $u(\Delta\omega,z,t)$ and $v(\Delta\omega,z,t)$ off resonance ($\Delta\omega\neq0$) through their mutual interactions with the $\mathcal{E}$ field. Integration of both sides of Eq. (22) from $t = -\infty$ to $t = +\infty \equiv T$, gives

$$\frac{d\vartheta(z)}{dz} = -\frac{2\pi\kappa\omega}{\eta c}\int_{-\infty}^{\infty}\int_{-\infty}^{\infty}\equiv T g(\Delta\omega)v(\Delta\omega,z,t)dtd(\Delta\omega), \qquad (31)$$

where the case $\theta(z) = A(z)$ will apply. The long time T signifies that the pulse $\mathcal{E}(z,t)$ has died away. This does not necessarily mean that the individual polarization components $u(\Delta\omega,z,t)$ and $v(\Delta\omega,z,t)$ have died away, but only that they destructively interfere to make the net polarization, given by Eq. (21), vanish because of the range of spectral frequencies $\Delta\omega$. Let $T = T_o + t'$, and choose $T_o$ as an arbitrary time origin having properties assigned to T above, with time $t'>0$ measured with respect to it. At $t = T$, Eqs. (24) and (25) (with $T_2' = \infty$) combine to give

$$u(\Delta\omega,z,t) = u(\Delta\omega,z,T_o)\cos(\Delta\omega t') + v(\Delta\omega,z,T_o)\sin(\Delta\omega t'). \qquad (32)$$

After substituting $v = (\partial u/\partial t)/\Delta\omega$ from Eq. (24) into Eq. (31), integrating Eq. (31) with respect to t, and applying Eq. (32), Eq. (31) becomes

$$\frac{d\theta(z)}{dz} = -\frac{2\pi\kappa\omega}{\eta n}\int_{-\infty}^{\infty}\left[\frac{g(\Delta\omega)}{\Delta\omega}\right]\left[u(\Delta\omega,z,T_o)\cos(\Delta\omega t') + v(\Delta\omega,z,T_o)\sin(\Delta\omega t')\right]d(\Delta\omega). \quad (33)$$

For arbitrarily large $t' \to \infty$ the contributions from the integrals in Eq. (33) occur only at $\Delta\omega=0$, since the integrands are oscillatory. Formally, the first integral in Eq. (33) appears to be undefined, and, therefore it is evaluated as the principle part of the integration in Eq. (31). The complex integration of $u(0,z,T_o)\int_{-\infty}^{\infty}\frac{\cos(\Delta\omega t')}{\Delta\omega}d(\Delta\omega)$ is then zero. Alternatively, one can argue that the first integral averages to zero for large T since $u(\Delta\omega,z)$ is an odd function, proportional to $\Delta\omega$ near $\Delta\omega=0$. The functions $g(\Delta\omega)$, v, and W are even functions of $\Delta\omega$. The second integral results in a delta function which allows v to contribute only at $\Delta\omega=0$ as follows:

$$\int_{-\infty}^{\infty}\frac{g(\Delta\omega)v(\Delta\omega,z,T_o)\sin(\Delta\omega t')}{\Delta\omega}d(\Delta\omega) = \pi g(0)v(0,z,T_o). \quad (34)$$

At $t = T_o$ according to Eq. (28),

$$v(0,z,T_o) = Np\,\sin\theta(z). \quad (35)$$

Therefore, from Eqs. (34) and (35), Eq. (33) yields

$$\frac{d\theta(z)}{dz} = -\frac{\alpha}{2}\sin\theta(z), \quad (36)$$

where $\alpha = \frac{8\pi^2 Np^2\omega g(0)}{\eta\hbar c}$.

At frequency $\omega$ the constant coefficient $\alpha$ in Eq. (36) is defined as the reciprocal absorption Beer's length for weak light pulses of narrow bandwidth, from coherent or incoherent sources, which do not

significantly alter the ground state population of the absorbing dipoles. This is signified by letting $\theta(z) \ll 1$ in Eq. (36). For this case the expression of Beer's law for an absorbing medium follows from Eq. (30) applied to (36), as

$$\mathcal{E}(z)^2 = \mathcal{E}(0)^2 e^{-\alpha z}. \tag{37}$$

The general solution of Eq. (36) is

$$\theta(z) = 2\tan^{-1}\{[\tan(\tfrac{1}{2}\theta_o)]\exp(-\tfrac{1}{2}\alpha z)\}, \tag{38}$$

which defines $\theta_o$ as the rotation angle of the fictitious vector $\underset{\sim}{P}(0,0,t)$ for those dipoles with $\Delta\omega=0$ and $z=0$ at the entry face plane of the medium. The branch solutions of $\theta$ versus z from Eq. (38) are plotted in Fig. (1-a). The solution for $\theta(z)$ is analytic, but we know of no analytical solutions for $\mathcal{E}(z,t)$ except particular ones which will be presented in the limit $\frac{d\theta}{dz} = 0$. Examples of computer plots for $\mathcal{E}$ versus z and t are shown in Fig. (1-b) for cases $\theta_o = 0.9\pi$ and $\theta_o = 1.1\pi$. The initial shapes $\mathcal{E}(0,t')$ are arbitrarily chosen to be Gaussian such that

$$\kappa \int_{-\infty}^{\infty} \mathcal{E}(0,t')dt' = \theta_o. \tag{39}$$

In Fig. (1) it is seen that the pulse area $\theta(z)$ diminishes toward $\theta(z) = 0$ for initially applied pulse areas $\theta_o < \pi$ if $\alpha$ is positive in Eq. (36), where Beer's law holds for $\theta(z) \ll 1$. If the sample is populated initially in the excited state, $\alpha$ is negative in Eq. (36), and $\theta(z)$ evolves by reading z as increasing from right to left in Fig. (1a). In this situation the amplifying medium will transform a small pulse of initial

area $\theta_o \ll \pi$ into a $\theta(z)=\pi$ pulse area independent of z for $z \gg \alpha^{-1}$ (this case, to be discussed later, is depicted in Fig. (8)). This property will hold if we maintain the ideal infinite plane wave condition with no variation of beam intensity in the x,y plane normal to the z direction. For $\tau > T_2^*$, and the area remaining at the value $\kappa\mathcal{E}_{max}\tau \sim \pi$, the area theorem would therefore demand that the amplified peak pulse $\tau$ continues to shorten. Losses would occur in a real case to limit the growth of power and the further shortening of $\tau$. Also any real beam profile is non-uniform in intensity. A uniquely defined field $\mathcal{E}(z,t)$ which is selected by a small aperture in the output will in general have a character which is influenced by neighboring portions of the beam, diffraction losses, initial beam focusing, beam self-focusing, off-resonance excitation etc. (which, for the present introductory discussion, are complications that cannot be predicted from Eq. (36) as it stands, whether or not damping is considered).

The deviations from linear pulse energy absorption rate are conveniently found from a computer evaluation of an empirical rate equation for the pulse energy T:

$$\frac{dT}{dz} = -\alpha T F(A,T,\text{"pulse shape"}), \tag{40}$$

where $$T = \frac{nc}{4\pi}\int_{-\infty}^{\infty}\mathcal{E}(z,t)^2 dt. \tag{41}$$

The function F is defined as a factor which is responsible for deviations from Beer's law. It is identified from the combination of Eqs. (22), (25), and (26) (with $T_1$, $T_2' = \infty$). The pulse shape can be defined

as an arbitrary smooth function, such as a Lorentzian or a Gaussian function. F will have minima near $A = \theta = 2\pi, 4\pi$ etc., and maxima near $3\pi$, $5\pi$ etc. because of the oscillatory behaviour ($W \sim -\cos\theta$) of dipoles near or at exact resonance. A pulse of small energy $\mathcal{T}$ and large width $\tau$ loses the same fractional amount of energy as does a more intense pulse of the same area but with a shorter width and a larger energy. This is a result of the relationship $\mathcal{T} \sim 1/\tau$ for fixed pulse area; i.e. the bandwidth of absorption by the pulse is proportional to its energy. Formally if the spectrum $g(\Delta\omega)$ is constant throughout the pulse spectrum, F does not depend upon $\mathcal{T}$ if the pulse area and shape are held constant. However, if the $g(\Delta\omega)$ spectrum is bell shaped and not flat, F then depends upon $\mathcal{T}$, and F will monotonically decrease with increasing $\mathcal{T}$. For $\mathcal{T}$ so large that the pulse width approaches or is less than $T_2^*$, a pulse may or may not become modulated with increasing distance z. If $\tau \gg T_2^*$ however, the induced polarization will last for a time comparable to $\tau$, and the pulse will retain a width comparable to its initial value and remain unmodulated by oscillations. This argument fails for $\theta > 3\pi$ because oscillations in the absorbed and emitted energy begin to split up the large area pulse into separate $2\pi$ pulses[10,17].

For a flat $g(\Delta\omega)$ spectrum the pulse shape and area dependence of F in Eq. (40) is plotted from computer calculations in Fig. (2) with the exception of the case of a square pulse shape. The factor F is precisely zero at $\theta = 2\pi$ for a $2\pi$ h.s. solution. This case is not plotted, but is almost undistinguishable from the Gaussian case except in the region of $\theta = 2\pi$. The square pulse result is analytic, given by

$F(A, \text{"square"}) = (1/A)\int_0^A dx J_0(x)$, which is obtained by solving Eq. (40) beginning with Eq. (22), in the usual way, and performing the required integration over $\Delta\omega$.

The Hyperbolic Secant Solution

We continue an outline of further predictions of Eqs. (36) and (38), and retain assumptions upon which they are based. For the system initially in the ground state ($\alpha$ positive) the dynamics of the pulse propagation presents a final stable situation which is not inherent in the amplifying case ($\alpha$ negative). Fig. (1b) shows how the $\theta_o = 1.1\pi$ pulse, above the critical area $\theta_o = \pi$, increases in area $[\theta(z) \sim \int \mathcal{E} dt]$ toward the limit $\theta(z) = 2\pi$, when $z \gg \alpha^{-1}$ and $\frac{d\theta}{dz} = 0$. While this increase in pulse area takes place the pulse loses some energy ($\sim \int \mathcal{E}^2 dt$) over a number of absorption lengths $\alpha^{-1}$, and appears to be reshaped into a stable form, which is presented as a hyperbolic secant traveling wave solution

$$\mathcal{E}(z,t) = \frac{2}{\kappa\tau} \operatorname{sech}[\frac{1}{\tau}(t-z/V)], \tag{42}$$

where $\kappa\int_{-\infty}^{\infty} \mathcal{E}(z,t')dt' = 2\pi$.

The solution Eq. (42) will be derived, and it will be seen that it is a unique analytical result[10] for a traveling wave pulse in the absence of dissipation ($T_1 = T_2' = \infty$) for a sharp line ($T_2^* = \infty$) at exact resonance. It serves as a solution in the case of arbitrary $g(\Delta\omega)$, but its uniqueness in this case has not been confirmed. Constant pulse velocity V and pulse width $\tau$ result when the depletion of energy from the first half of the pulse ($-\infty \leq t \leq z/V$) by the absorbing two level system is exactly balanced by

emission of the same amount of energy by the system into the second half of the pulse ($z/V \leq t \leq \infty$). During its second half the pulse is amplified by that portion of the two level system which the pulse had previously pumped into the excited state during its first half. This has the effect of producing a pulse delay, making $V < c/\eta$.

Sharp Line Case

In view of the indications of our initial computer calculations[11], we are led to believe that a traveling wave pulse exists which is at resonance with the two level system and has a pulse area of $2\pi$. Such a pulse solution must therefore satisfy the equations

$$\frac{\partial \mathcal{E}}{\partial z} = -\frac{1}{V}\frac{\partial \mathcal{E}}{\partial t} = -\frac{2\pi\omega}{\eta c}\int_{-\infty}^{\infty} g(\Delta\omega)v(\Delta\omega,z,t)d(\Delta\omega) - \frac{\eta}{c}\frac{\partial \mathcal{E}}{\partial t}, \tag{43}$$

one of which is Eq. (22). Our task is to find the proper pulse shape which satisfies the Eqs. (18) and (43). Let $g(\Delta\omega) = \delta(\Delta\omega)$ be a delta function in Eq. (43), and substitute into Eq. (43) the polarization given by $v(0,z,t)$ from Eq. (28). Therefore

$$\frac{\partial \mathcal{E}}{\partial t} = \left(\frac{2\pi\omega Np}{\eta c}\sin\varphi\right)\Big/\left(\frac{1}{V} - \frac{\eta}{c}\right). \tag{44}$$

The expression

$$\frac{\partial \varphi}{\partial t} = \kappa\mathcal{E} \tag{45}$$

from Eq. (30) is applied to Eq. (44), giving the relations

$$\mathcal{E} = \frac{2}{\kappa T}\sin\varphi/2 \tag{46}$$

and

$$\frac{\partial^2\varphi}{\partial t^2} = \left(\frac{1}{\tau^2}\right)\sin\varphi, \tag{47}$$

where $1/V = \frac{2\pi\kappa\omega N p\tau^2}{\eta c} + \eta/c$. Eq. (47) is recognized as the equation which governs the motion of a pendulum initially oriented in the non-equilibrium position $\varphi_o = \pi$. From a number of possible solutions to Eq. (47), only one of them is of particular importance to the transparency effect. It is obtained by writing Eq. (46) in terms of $q = \kappa\mathcal{E}\tau/2$, and combining Eq. (46) with Eq. (44) to give $\dot{q} = (q/\tau)\sqrt{1-q^2}$ or $dt/\tau = \frac{dq}{q\sqrt{1-q^2}} = d(\text{sech}^{-1}q)$. This leads to the $2\pi$ h.s. solution, expressed by Eq. (42), which must be of finite pulse energy. The equivalent of Eq. (42), expressed as the solution of the pendulum equation (Eq. (47)), is

$$\varphi = 4\tan^{-1}\left\{e^{\frac{1}{\tau}(t - \frac{z}{V})}\right\}, \tag{48}$$

which corresponds to the pendulum oscillation of infinite period. The other pendulum solutions, corresponding to period swings or oscillations which have $\int_{-\infty}^{\infty}(\frac{\partial\varphi}{\partial t})^2 dt = \infty$ (see Fig. 3), are rejected as corresponding to light pulses of infinite energy. A number of pendulum solutions have been discussed by Jaynes[6] and Cummings relative to a maser cavity problem in which a two level system is at resonance with a microwave field. Bloembergen and Pound[6] and Bloom[6] discuss the standing wave radiation damping problem for the loss of magnetization of a precessing macroscopic magnetic moment while it is coupled to a resonance LCR tuned circuit. Bloom shows in some detail the nature of the hyperbolic secant radiation damping of nuclear magnetism as a function of cavity losses. Dicke[6] obtains a similar solution for the transient behaviour of a radiating macroscopic electric dipole moment in a standing microwave cavity problem.

Case of Inhomogeneous Broadening

If we assert that a symmetric $2\pi$ h.s. pulse is supported by an inhomogeneously broadened medium, then each off-resonant component $v(\Delta\omega,z,t)$ in Eq. (43) is expected to respond symmetrically in time with respect to the h.s. pulse. It will be shown that it is consistent to define

$$v(\Delta\omega,z,t) = v(0,z,t)f(\Delta\omega), \tag{49}$$

where $f(\Delta\omega)$ is some even function of $\Delta\omega$ independent of t, with $f(0)=1$. If Eq. (49) is valid, then the spectral integration of $f(\Delta\omega)$ in Eq. (43) will lead to Eq. (44), apart from a constant factor, and Eq. (44) in turn leads to the $2\pi$ h.s. solution as shown. The form of $f(\Delta\omega)$ is obtained by solving Eqs. (25) and (26) for $u(\Delta\omega,t)$ and $W(\Delta\omega,t)$, with $T_1 = T_2' = \infty$, and using Eqs. (28) and (49). Eq. (24) then yields

$$\frac{1-f(\Delta\omega)}{\Delta\omega^2 f(\Delta\omega)} = \frac{1}{\dot{\varphi}}\int_{-\infty}^{t} \sin\varphi(t')dt' = \tau^2, \tag{50}$$

where $\tau^2$ for a given z is independent of t and $\Delta\omega$, because $f(\Delta\omega)$ and $\varphi$ are respectively independent of t and $\Delta\omega$. The second of Eqs. (50) yields

$$f(\Delta\omega) = \frac{1}{1+\Delta\omega^2\tau^2}\ ; \tag{51}$$

and the first equation, using Eq. (45), gives the pendulum equation Eq. (47). The parameter $\tau$ must be a constant independent of z if the traveling wave solution Eq. (48) to the pendulum equation, together with Eq. (45), is to satisfy Maxwell's Eq. (43).

Hyperbolic Secant Pulse Properties

During the evolution of the pulse toward the hyperbolic secant form the pulse shape changes while net energy is being absorbed by the two level

system. Computer plots in Fig. (4) show examples of pulse energy absorption as a function of pulse area $A=\theta$ for fixed positions z. Pulses which are not hyperbolic secant in shape will leave the undamped inhomogeneously broadened system excited to some extent and therefore lose energy by an amount $\Delta W = -\frac{dT}{dz} = N\hbar\omega/2 + \int_{-\infty}^{\infty} W(z,\Delta\omega,t=\infty)g(\Delta\omega)d(\Delta\omega)$, which follows upon combining Eqs. (22), (26) and (41). At $\theta = 2\pi$ the hyperbolic secant pulse gives $\Delta W = 0$ regardless of the spectral shape of $g(\Delta\omega)$. This implies that u, v, and W in the limit of no damping start from their ground state values of 0, 0, $-\frac{N\hbar\omega}{2}$ respectively and return precisely to these same values after the $2\pi$ pulse subsides, <u>independently</u> of the off-resonance parameter $\Delta\omega$ to which the vector $\underset{\sim}{P}$ (Eq. (17)) is assigned. Fig. (5) shows the trajectory of the end point of vector $\underset{\sim}{P}$ for various values of $\Delta\omega\tau$. From the analysis relating to Eqs. (49) and (51) the components of $\underset{\sim}{P}$ are found to be

$$u(\Delta\omega,z,t) = \frac{2Np\ \Delta\omega\tau\ \sin(\varphi/2)}{1+(\Delta\omega\tau)^2}, \tag{52}$$

$$v(\Delta\omega,z,t) = \frac{Np\sin\varphi}{1+(\Delta\omega\tau)^2}, \tag{53}$$

and

$$W(\Delta\omega,z,t) = \frac{N\hbar\omega}{2}\left(\frac{2\sin^2(\varphi/2)}{1+(\Delta\omega\tau)^2} - 1\right), \tag{54}$$

where $\varphi$ is given by Eqs. (30) or (48), so that

$$\sin(\varphi/2) = \operatorname{sech}\left[\frac{1}{\tau}(1 - z/V)\right]. \tag{55}$$

From Eqs. (22), (43), and (53) the general expression for the reciprocal pulse velocity is

$$V^{-1} = \eta/c + \frac{\alpha\tau^2}{2\pi g(0)}\int_{-\infty}^{\infty}\frac{g(\Delta\omega)d(\Delta\omega)}{1+(\Delta\omega\tau)^2}, \tag{56}$$

which reduces to the time delay per cm of $V^{-1} \cong \alpha\tau/2$ in the limits $T_2^* \ll \tau$, $\alpha\tau \gg \eta/c$, where $g(\Delta\omega)$ is assumed constant over a spectral region defined about $\sim \frac{1}{\tau}$. These conditions indicate that the pulse is retarded in time about a pulse width $\tau$ per absorption length $\alpha^{-1}$.

If a $2\pi$ hyperbolic secant pulse is injected into the target sample at z=0, the spectral function $g(\Delta\omega)$ can be of any non-symmetrical shape, and ideal self-induced transparency will operate immediately. Therefore the special results for the $2\pi$ pulse above apply upon substituting Eq. (52) into Eq. (23), to give a phase shift linear with distance and independent of time, expressed by

$$\frac{d\phi(z)}{dz} = k' = \frac{\alpha\tau^2}{2\pi g(0)} \int_{-\infty}^{\infty} \frac{\Delta\omega g(\Delta\omega) d(\Delta\omega)}{1+(\Delta\omega\tau)^2} . \qquad (57)$$

Consequently the resonance process alters the wave vector in the resonant medium from the value k as seen from Eq. (1), to the value (k+k'). For $\tau \gg T_2^*$, Eq. (57) reduces to the ordinary result for linear dispersion.

The uniqueness of the $2\pi$ h.s. solution in the narrow line case $(g(\Delta\omega) = \delta(\Delta\omega))$ is now argued as follows. Out of a general class of traveling wave solutions S of the form $S(t - \frac{z}{V})$, we note first that the $2\pi$ h.s. solution is one in a class of pendulum solutions which is a solution also to the cavity problem, where all of these solutions namely the pendulum solutions of Eq. (47) with k' given by Eq. (57). to the cavity problem are known. By the cavity problem it is meant that S is a solution to the second of the two equations in Eq. (43), where only the time dependence is involved. As a cavity solution, the $2\pi$ h.s. function is a solution of the undamped two level system (as in an NMR experiment), as shown by Eqs. (52), (53) and (54), which applies to both on and off-resonance behaviour. The $2\pi$ h.s. solution contains all the parameters necessary to describe any set of initial conditions in the cavity problem.

The $2\pi$ h.s. function is unique out of all the cavity problem solutions in that it is the only pulse solution of finite energy, required by self-induced transparency, which satisfies simultaneously both the traveling wave (first) and cavity (second) equations of Eq. (43).

Actual experimental results indicate that nearly symmetrical hyperbolic secant-like pulse shapes grow even if $g(\Delta\omega)$ is not excited symmetrically. The tendency to produce spectrally clean and nearly symmetric output transparency pulses is associated with the excitation of $g(\Delta\omega)$ at any $\Delta\omega$ if $g(\Delta\omega)$ presents a broad line width with a slowly varying derivative $d[g(\Delta\omega)]/d(\Delta\omega)$. If the pulse width $\tau$ is sufficiently large, $g(\Delta\omega)$ will appear to be nearly a flat distribution in first order, because it is excited over a very narrow spectrum. A second order correction will arise as a small change in the effective host medium refractive index because of the dispersion contributed by a small imbalance of off-resonance dipoles which give $g(\Delta\omega)$ a slight asymmetry about $\Delta\omega=0$.

## III. CHANGES IN SELF-INDUCED TRANSPARENCY PULSE CHARACTERISTICS WITH DISTANCE

There are a number of factors always present in the experiment which actually cause the pulse to change shape and broaden, attenuate, self-focus or defocus, or perhaps even to sharpen, depending upon a variety of actual experimental conditions. It is instructive first to discuss some qualitative features of the pulse before it becomes delayed and shaped into a stable hyperbolic secant form.

At a given position z, let t(z) define a time point during the pulse which corresponds approximately to the same point on the pulse at other positions z, chosen to define a certain pulse characteristic such as maximum amplitude or slope of $\mathcal{E}(t(z),z)$. Then t(z) is some function of z, and if it is applied as a limit in the integration of Eq. (22), one must take this into account in carrying out the differentiation process with respect to z. Therefore

$$\int_{-\infty}^{t(z)} \frac{\partial \mathcal{E}}{\partial z}(t',z)dt' = \frac{\partial}{\partial z}\left(\int_{-\infty}^{t(z)} \mathcal{E}(t',z)dt'\right) - \frac{\partial t(z)}{\partial z}\mathcal{E}(t(z),z). \tag{58}$$

Define

$$\frac{\partial t(z)}{\partial z} = \eta/c + \frac{1}{V(t(z))} \text{ ; and} \tag{59}$$

$$\frac{1}{V(t(z))} = \left[1/\mathcal{E}(t(z),z)\right]\left[\frac{2\pi\omega}{\eta c}\int_{-\infty}^{t(z)}\int_{-\infty}^{\infty} g(\Delta\omega)v(\Delta\omega,t',z)d(\Delta\omega)dt' + \frac{1}{\kappa}\frac{\partial\varphi(t(z))}{\partial z}\right], \tag{60}$$

where $\varphi(t(z))$ is expressed by Eq. (30), with t replaced by t(z), and $\frac{\partial t(z)}{\partial z}$ is the reciprocal of the instantaneous pulse velocity at t(z).

The resonance process contributes $1/V(t(z))$ as a component of the reciprocal pulse velocity. The pulse shape changes in distance and time, and the velocity $V(t(z))$ is altered over several absorption Beer's lengths $\alpha^{-1}$.

Varying Pulse Delay

In the case of $\theta_o = 1.1\pi$, as seen from Fig. (1b), the pulse delay increases with increasing z in the z,t plane, and acquires a constant pulse velocity V, or constant delay time $T = \alpha\tau/2$ per unit length relative to the retarded time $t-\eta z/c$, where $\tau$ is the final stable pulse width. For the two level system initially in the ground state, Eq. (60) displays the following pulse area properties shown in Fig (1b), where $t(z)$ is defined at the pulse maximum.

For $2\pi > \theta_o > \pi$:

As $\theta \to 2\pi$, $V(t(z)) > V$ and $\frac{\partial\varphi}{\partial z} > 0$. When $\theta = 2\pi$, $V(t(z)) = V = (\frac{\alpha\tau}{2})^{-1}$, $t(z) = t + z/V$, and $\frac{\partial\varphi}{\partial z} = 0$ for $z \gg \alpha^{-1}$.

For $\theta_o < \pi$:

As $\theta \to 0$, $1/V(t(z)) \ll \eta/c$ and $\frac{\partial\varphi}{\partial z} < 0$.

As seen in Fig. (1b), for the initial pulse conditions $\theta_o = 0.9\pi$, the absorbed pulse exhibits little or no delay $V(t(z))^{-1}$ per unit length, because $\frac{\partial\varphi}{\partial z}$, as a negative quantity in Eq. (60) , cancels out the double integral term to a large extent. In the limit of low pulse power absorption, where $\varphi$ is small, $v \propto \mathcal{E}$, and $\kappa\mathcal{E}\tau \ll 1$, whereupon $V(t(z))^{-1} \approx 0$. The leading edge of the pulse is absorbed linearly and its rise time is altered very little. However, for larger $\varphi$, corresponding to large $t(z)$ for the same z, the lagging edge of the pulse is in fact stretched out because it is amplified briefly by the contribution of off-resonance

dipole radiation. By multiplying numerator and denominator of the double integral term in Eq. (60) by $\mathcal{E}^2$, setting $V(t(z))^{-1} = 0$, and defining $d\varphi = \kappa\mathcal{E}dt$, therefore,

$$\frac{\partial\varphi}{\partial z} = -\frac{\alpha}{2}\varphi. \tag{61}$$

This describes the limit of classical low power absorption where

$$\alpha = \left(\int_{-\infty}^{\infty} g(\Delta\omega)\nu\mathcal{E}\omega\, d\Delta\omega\right) \Big/ \left(\frac{\eta c\mathcal{E}^2}{4\pi}\right)$$

expresses the ratio of the integrated power loss $\frac{dW}{dt}$ (Eq. (26)) with $T_1 = \infty$) to the average energy flux $\eta c\mathcal{E}^2/4\pi$ of the circularly polarized pulse.

For the two level system initially in the excited state, the double integral in Eq. (60) becomes a negative term, because $g(\Delta\omega)$ is inverted. The term $\frac{\partial\varphi}{\partial z}$ remains positive, as dictated by the area theorem of Eq. (36), and a small pulse with initial $\theta_o < \pi$ is amplified toward $\theta = \pi$ for $z \gg \alpha^{-1}$, where $\alpha$ is negative. Now the leading edge of the pulse is sharpened by the initial gain. After the effective gain factor $|\alpha F|$ (Eq. (40)) sharply decreases in magnitude the lagging edge of the pulse falls and stretches out. While the pulse is being formed and amplified at any z, we cannot formulate a general analytic shape for $\mathcal{E}$ which compares to the $2\pi$ h.s. case for transparency. However, one must deduce, as the $\pi$ pulse continues to be amplified, that the double integral term in Eq. (60) is negative, $\frac{\partial\varphi}{\partial z} \to 0$, and $V(t(z)) \leq 0$.

This expression for the pulse velocity gives the appearance that

the actual pulse velocity exceeds $c/\eta$.

But the pulse velocity as defined here is only an arbitrary definition of the backward displacement in time versus distance (hence $V(t(z))$ is negative) of some pulse shape characteristic, and not of the speed of light itself. The pulse velocity increase implies a sharpening of the leading edge of the pulse because of the amplification process. Therefore, the peak of the pulse rises rapidly with increasing z and appears earlier in time t, as shown in a special case relating to Fig. (4), to be discussed later. Actually a noise impulse will signify the first appearance of $\mathcal{E}$, and the leading edge of the amplified pulse can never recede to a time earlier than $t_o + z\eta/c$, which is the earliest permissible time that information can be conveyed to an observer at position z by the first noise impulse generated earlier at time $t_o$.

Although the hyperbolic secant function (Eq. (42)) for $\mathcal{E}$ has been introduced as an analytic pulse solution to the self-induced transparency pulse field, this function at $t = -\infty$ behaves in contradiction to the requirement of causality. This lack of causality is introduced because of the assumptions used in deriving Eq. (42). However Eq. (42) is physically acceptable as a basis of analysis since it accurately represents the shape of $\mathcal{E}$ for finite times t.

Multiple Pulse Formation

The area theorem expressed by Eq. (36) implies that any initial pulse area $\theta_o$, which obeys the condition $(n+1)\pi > \theta_o > n\pi$, will increase in area toward $(n+1)\pi$ if n is odd, or it will decrease in area toward $n\pi$ if n is even, and the pulse sharpens to give an increase in pulse power. Figs. (1b) and (6) respectively show the results of computer plots of pulse shape changes for the cases $2\pi > \theta_o > \pi$ and $3\pi > \theta_o > 2\pi$. If the

initial pulse is to evolve into an area which is an integer multiple of $2\pi$, it may in general split up into n separate $2\pi$ pulses which do not overlap one another at sufficiently large z. Fig. (7) gives computer plots which show how two separate $2\pi$ pulses emerge in a distance $z \gtrsim \alpha^{-1}$ from input pulses $\theta_o$ near $4\pi$. Each $2\pi$ pulse has its own particular width and corresponding delay time proportional to the pulse width. Therefore, the narrower pulse always occurs earlier at the output. Fig. (16-c), to be discussed later, shows the observed output of what could possibly be a pulse splitting effect of this type in a ruby excited self-induced transparency experiment. G. L. Lamb[17] has analyzed a special case of this pulse "splitting effect" phenomenon under the assumption that a narrow line ($T_2^* = T_2' = \infty$) two level system remains stable, but it is not known that this splitting effect applies to the case of inhomogeneous broadening. The manner in which the computed pulse splitting occurs depends upon the initial pulse shapes. Here a flat two level inhomogeneous spectrum with $T_2' = \infty$ is excited with pulses of Gaussian shape. As the pulses separate completely they evolve into individual hyperbolic secant pulses with separate areas of $2\pi$.

Pulse Stripping, Superposition, and Self-Focusing

In the actual experimental situation the pulse entering into the resonant medium is not uniform in intensity across its profile. For any position z in the sample we visualize for convenience that the pulse intensity falls off symmetrically as some function of the radius r, measured normal to z and outward from an axis in the rod.

If we assume that the plane wave analysis of the transparency effect is applicable to small patches of the light wave front anywhere on the profile, a modification of the pulse intensity output across the beam profile can be described along the rod. At a particular radius $r \gtrsim r_c$, where the pulse area falls below $\pi$, the light will be absorbed for all $r > r_c$

within a few Beer's lengths $\alpha^{-1}$. Consequently, the outer periphery of the original pencil of light should be stripped away. A core remains which contains a distribution of pulse areas with each pulse area approaching $2\pi$. These have their own pulse widths and delay times corresponding to the intensity assigned to each region at $r < r_c$. The more intense beam centered about $r = 0$ will reach the exit end of the rod in a certain time before the arrival time of the portion of the beam distributed at $r \sim r_c$, so that a form of "do-nut" shaped intensity profile remaining near the entry end of the rod would be expected on this basis. The strong variation of delay with input intensity near $r = r_c$ would prevent the formation of sharp outer edges in the intensity profile. Also, diffraction will couple energy from the beam at a given radius $r_1$ to a different radius $r_2$ at a distance further down the rod. The transparency effect must be analyzed in more detail to take these effects into account. Our initial investigation of the effects of these additional complications by analytic methods have been unfruitful.

If effects caused by diffraction and stripping can be ignored, particularly if the beam intensity falls off very slowly from $r = 0$, the pulse intensity output $\mathcal{E}^2$ versus time t, as displayed from a photodiode, can be visualized as a superposition of squares of individual hyperbolic secant curves, where each curve is delayed by an amount proportional to its own pulse width $\tau$. The total superposition of hyperbolic secant functions would tend to display a skewed asymmetric pulse when the beam is detected over a large aperture at the target output. Use of a sufficiently small aperture would give a uniform bell shaped function approaching the h.s. shape.

Suppose the output electric field profile is given as

$$\mathcal{E}(r,t) = \frac{2}{\kappa\tau(r)} \operatorname{sech}\left\{\frac{1}{\tau(r)}(t - t_o(r))\right\},$$

where $\tau(r)$ is the $2\pi$ h.s. pulse width at radius r as defined by $\tau$ in Eq. (42), and $t_o(r)$ is the time of the output pulse peak at radius r and distance z. The observed electric field intensity $\mathcal{E}_T^2$ from an aperture with radius $r_c$ at the end of the rod of length z = L is proportional to

$$\mathcal{E}_T^2(t) \sim \int_{r=0}^{r=r_c} \frac{1}{\tau(r)^2} \operatorname{sech}^2\left\{\frac{t}{\tau(r)} - \alpha L/2\right\} r\,dr. \qquad (62)$$

The experimental measurements of pulse areas, to be discussed later, could show deviations from the ideal $2\pi$ h.s. case, partly because of the superposition effect indicated by Eq. (62). Depending upon the exact form of $\tau(r)$, $t_o(r)$, and the aperture size $r_c$, the measured pulse areas could be either greater or less than $2\pi$ because of the above effect.

An additional transverse effect is indicated by the dependence of $\frac{d\phi}{dz}$, given by Eq. (57), upon the pulse width $\tau$. A self-focusing property can be assigned to the light beam according to Huygens principle if $\frac{d\phi}{dz}$ increases with increasing peak field $\mathcal{E}_o(r) = 2/\kappa\tau(r)$, which is equivalent to an increasing pulse energy or decreasing $\tau(r)$ for a $2\pi$ h.s. pulse. This will occur if the applied frequency $\omega$ is on the high frequency side of the resonance line ($\Delta\omega$ negative), and the phase velocity $\omega/(k+k'(r))$ of the periphery of the beam exceeds that of the center of the beam. This focusing effect will produce an instability which modifies the plane wave $2\pi$ h.s. expression for $\frac{d\varphi}{dz}$ given by Eq. (57) to an unknown form.

Conversely, if the applied frequency $\omega$ is on the low frequency side of the resonance peak ($\Delta\omega$ positive), a different type of defocusing process will occur. The simultaneous existence of self-focusing, pulse stripping, and diffraction makes it questionable to consider these effects as independent of one another. The detailed nature of transverse beam behaviour here remains to be worked out.

Effect of a Transverse Mode on Self-Induced Transparency

If the electromagnetic field is forced to propagate in a single mode, as in the transmission of a pulse down a wave guide, or by the maintenance of a transverse Gaussian profile of laser light down a cylinder, the area theorem (Eq. (36)) must be modified to take this property into account. Consider a dispersionless wave guide which contains a uniformly inverted two level amplifying medium, which restricts pulse transmission to a single mode expressed by a complex orthogonal mode described by the function $\underset{\sim}{\xi}(x,y)$. The electric field expressed by Eq. (19) is then written as

$$\underset{\sim}{E}(x,y,z,t) = \underset{\sim}{\xi}(x,y)\mathcal{E}(z,t)e^{i[\omega t-kz-\phi(z)]} + c.c. \tag{63}$$

Therefore in place of Eq. (22) the formal method[18] for introducing single mode behaviour in Maxwell's equations results in the expression

$$\frac{\partial \mathcal{E}'}{\partial z} = -\frac{\eta}{c}\frac{\partial \mathcal{E}'}{\partial t} + \frac{\left(\frac{2\pi\omega i}{\eta c}\right)\iint_{xy} dxdy\left[\underset{\sim}{\xi}^*(x,y)\cdot\hat{p}\right]P_+(x,y,z,t)e^{-i[\omega t-kz]}}{\int_x\int_y|\underset{\sim}{\xi}(x,y)|^2dxdy} - \frac{\beta}{2}$$

where a loss term $\beta\mathcal{E}'/2$ is introduced $\mathcal{E}' = \mathcal{E}e^{-i\phi(z)}$, $P_+(x,y,z,t)$ is by the form of Eq. (21), and $\eta$ now takes into account the presence of the wave guide.

The mode function $\underset{\sim}{\xi}(x,y)$ is normalized so that $\hat{p} \cdot \underset{\sim}{\xi}(0,0) = 1$ at the center of the beam, where $\hat{p} = \frac{\langle \psi_2^* | \underset{\sim}{p}_o | \psi_1 \rangle}{|\langle \psi_2^* | \underset{\sim}{p}_o | \psi_1 \rangle|}$. In Eq. (64) the phase factor inherent in $\underset{\sim}{\xi}(x,y)$ is cancelled by its complex conjugate which occurs in $\underset{\sim}{\xi}(x,y) \cdot \hat{p}$. For the amplifying medium the modified area theorem equation for the pulse area $A(z)$ at the beam center ($x = y = 0$) becomes

$$\frac{dA(z)}{dz} = + \frac{\frac{\alpha}{2}\int_x\int_y dxdy\left[\hat{p} \cdot \underset{\sim}{\xi}^*(x,y)\right]\sin\left\{A(z)\left[\hat{p} \cdot \underset{\sim}{\xi}^*(x,y)\right]\right\}}{\int_x\int_y dxdy\left[\hat{p} \cdot \underset{\sim}{\xi}^*(x,y)\right]^2} - \frac{\beta}{2}A(z), \quad (65)$$

where $\alpha$ is the linear resonant gain constant for this particular mode. The tipping angle of vector $\underset{\sim}{P}$ is given by $A(z) = \theta(z)$ only at the center of the beam. In effect the electric field at $x = y = 0$ is determined by its functional variation imposed by the mode function $\underset{\sim}{\xi}(x,y)$; and the dipoles at a particular transverse x,y position obey the torque type equation (Eq. (18)) when driven by the electric field $\underset{\sim}{\xi}(x,y)\mathcal{E}(z,t)$ at that position. The net area derivative at $x = y = 0$ in Eq. (65) is therefore determined by the functional variation of $\underset{\sim}{\xi}(x,y)$ over all x,y. By this procedure the constraint imposed by the "wave guide mode" bypasses the problem of diffraction, but at the expense of assuming that the $\underset{\sim}{\xi}(x,y)$ function holds throughout the evolution of the pulse area A with distance z. Nevertheless, consideration of the relation Eq. (65) is much more realistic with regard to questions posed in the literature[19] regarding the production of "$\pi$ pulses" by laser amplifiers. In these experiments there are large transverse variations in field intensity, and the pseudo vector tipping angle has a strong dependence on transverse x,y position in the beam.

Let Eq. (65) carry over to the case of a single transverse mode traveling wave laser. Assume a specific Gaussian transverse function

$\underset{\sim}{\xi}^{*}\hat{p} \sim \exp\left[-(x^2 + y^2)/r_o^2\right]$, where $r_o$ is some mean transverse distance. Then Eq. (65) reduces to

$$\frac{dA}{dz} = \frac{\alpha}{A}(1-\cos A) - \beta A/2. \tag{66}$$

The equilibrium area $A \cong \cos^{-1}(1 - 2\beta A/\alpha)^2$ shows that in the limit of small losses ($\beta \to 0$), $A \to 2\pi$ in the laser amplification process. In the plane wave case it is popularly expected that $A \to \pi$ but the existence of the chosen transverse mode and definition of pulse area here happens to yield $A = 2\pi$. If losses expressed by the parameter $\beta$ or $\beta/\alpha$ increase in Eq. (66), the corresponding pulse area becomes less than $2\pi$. Thus far the pulse area referred to is the exact resonance tipping angle $\theta(z)$ at the exact center of the beam profile, where a small aperture is presumed to monitor it. If the entire beam profile is measured, the apparent pulse area is modified considerably from its value at the center of the beam to an apparent value which may be different from $2\pi$, depending upon the means of averaging. Of course this analysis is to be taken only in a qualitative sense, because the equation which should apply is sensitive to the mode function $\xi(x,y)$ which is actually present. For example if we choose $\underset{\sim}{\xi}^{*}\hat{p} \approx \frac{1}{1+(x^2+y^2)/r_o^2}$ the area theorem would be given by

$$\frac{dA}{dz} = \frac{\alpha}{2}\left[\int_0^A \frac{\sin y\, dy}{y}\right] - \frac{\beta A}{2}, \tag{67}$$

where the integral function above is the sine integral function $\mathrm{Si}(y)$. Here the equilibrium area A for finite $\beta$ is entirely different from the previous case, and for no loss ($\beta=0$) the equilibrium area A is indefinitely large.

Orientation and Degeneracy Effects

So far the analysis of self-induced transparency has assumed that all dipole matrix elements are singularly defined for a simple two level system, and that the dipoles are oriented in a common direction throughout the sample. In a gas the direction of light polarization of a plane wave will specify a corresponding dipole moment polarization direction at any time if the induced dipole moment is obtained from the excitation of ground symmetric states. There are cases,[20] however, in which the induced dipole moment will not occur in a unique direction specified by the applied field; instead, there may exist projections of dipole moment matrix elements upon the incident optical field polarization direction which are nearly random in value.

An instructive way to look at the above problem is to say that the dipole moments are apparently different for different molecular orientations. This can be illustrated by a simple example in which two independent dipole species with dipole matrix elements $p_1$ and $p_2$ interact independently with a light pulse. Here $p_1$ and $p_2$ are not randomly oriented but are each polarized in the same direction. Only one mode of electric field polarization will result, and the previous area theorem analysis can be applied to give

$$\frac{dA}{dz} = -(\alpha_1/2)\sin A - \frac{p_1\alpha_2}{2p_2}\sin[(p_2/p_1)A]. \tag{68}$$

The pulse area is defined as $A = \theta_1$, so that $\theta_2 = (p_2/p_1)A$, and $\alpha_1$ and $\alpha_2$ are the absorption coefficients for each type of dipole. Eq. (68) must reduce to $\frac{dA}{dz} = -\frac{1}{2}(\alpha_1+\alpha_2)A$ for A small. For $\frac{dA}{dz} = 0$, the pulse

area will no longer be at $2\pi$. For $(p_1\alpha_2)/p_2 \ll \alpha_1$, the species $p_1$ will dominate, and to first order in $p_1\alpha_2/(p_2\alpha_1)$ a stable pulse area

$$A = 2\pi - \frac{p_1\alpha_2}{p_2\alpha_1}\sin\left(\frac{p_2}{p_1}\,2\pi\right)$$

will result.

Now consider gas molecules in which the dipole moment p is induced only along a particular molecular axis. For linearly polarized light let $\Omega$ denote the angle between $\underset{\sim}{\mathcal{E}}$ and $\underset{\sim}{p}$, so that the effective field acting on the dipole is $E\cos\Omega$. An equivalent of this projection procedure is to specify that the effective dipole moment $p_{eff} = p\cos\Omega$ interacts with $\mathcal{E}$. Hence the area theorem is derived for such a system by summing over all possible values of $p_{eff}$ which interact with the uniquely determined field $\mathcal{E}$ which is a consequence of the sum of all the dipole interactions. Let the pulse area A be defined as the tipping angle at resonance for all dipoles with $\Omega = 0$. The area derivative with respect to distance, as expressed by Eq. (36), becomes the sum of all $\sin\left(\frac{p_{eff}A}{p}\right)$ contributions over a unit sphere, expressed as

$$\frac{dA}{dz} = -\left(\frac{3\alpha}{2}\right)\int_0^{\pi} \sin\Omega\cos\Omega\sin(A\cos\Omega)\,d\Omega = -\left(\frac{3\alpha}{2A^2}\right)(\sin A - A\cos A). \qquad (69)$$

The separate $\cos\Omega$ factor in the integral expresses the reprojection of the field radiated by $p_{eff}$ back onto the applied field $\mathcal{E}$. Eq. (69) indicates that no stable pulse condition exists in which complete transparency occurs. If circularly polarized light is applied instead of linearly polarized light, then with $\Omega = \cos^{-1}(p_{eff}/p)$ defined as the angle between the polarization direction and the propagation direction,

$$\frac{dA}{dz} = -\frac{3\alpha}{8}\int_0^{\pi} \sin^2\Omega \sin(A\sin\Omega)\,d\Omega$$

$$= -\frac{\alpha}{2} J_1(A) + \frac{\alpha}{10} J_3(a) + \frac{3\alpha}{2}\sum_{n=2}^{\infty} \frac{J_{2n+1}(A)}{(2n-1)(2n+1)(2n+3)}\,, \qquad (70)$$

where $J_n(A)$ is the Bessel function[21] of order n, finite at A=0. In the limit of small A, Eqs. (69) and (70) reduce to the linear limit which requires that $\frac{dA}{dz} = -\frac{\alpha}{2}A$.

For a rigorous quantum description of orientation effects as they affect transparency in a gas, the problem must be expressed in terms of angular momentum states. Suppose the ground and excited states are characterized respectively by a multiplicity of 2J + 1 and 2J' + 1, with angular momenta J and J'. The dipole matrix elements involving transitions between such states have been cataloged[22]. Generally, the contribution to the pulse area derivative dA/dz (assuming equal initial ground state populations) from allowed transitions between the states $|J,m_J\rangle$ and $|J',m_{J'}\rangle$ is proportional to $|p(m_J,m_{J'})|\sin\left\{|p(m_J,m_{J'})|A/p_o\right\}$, for the same reasons leading to Eq. (36), where $|p(m_J,m_{J'})|$ is defined as the dipole matrix element for the transitions $m_J \leftrightarrow m_{J'}$. The matrix elements are assumed to refer to either $\pi$ optical transitions, or $\sigma\pm$ optical transitions. The dipole factor $p_o$ is formally arbitrary, but to be specific it is chosen to be the largest of the $|p(m_J,m_{J'})|$ involved. Generally the pulse area derivative may be written as

$$\frac{dA}{dz} = -\frac{p_o\alpha}{2}\,\frac{\sum |p(m_J,m_{J'})|\sin\left\{|p(m_J,m_{J'})|A/p_o\right\}}{\sum |p(m_J,m_{J'})|^2}\,, \qquad (71)$$

which is derived in the same way as Eq. (36). The summation is over $m_J$ and $m_{J'}$, restricted either to all $\sigma\pm$ transitions or to all $\pi$ transitions,

where each of $m_J$ and $m_{J'}$ can appear only once in the summation. The factor $\alpha$ from Eq. (36) is defined here with $p^2$ replaced by $\sum |p(m_J,m_{J'})|^2$, and $A = \frac{2p_o}{\hbar} \int_{-\infty}^{\infty} \mathcal{E}(z,t')dt'$.

Referring to the tabulated matrix elements[22], the numbers $|p(m_J,m_{J'})|$ are either zero, or equal to $p_o$, for $\pi$ and $\sigma$ transitions if J=0, J'=1; J=J'=1; J=1, J'=0; or J=J'=$\frac{1}{2}$. For these transitions the above formula reduces to $-\frac{1}{2}\alpha\sin A$ for which $2\pi$ h.s. pulses should be formed and display the transparency effect. The same remarks apply to $\pi$ transitions for J=$\frac{1}{2}$, J'=3/2 or vice versa. But for J=$\frac{1}{2}$, J'=3/2, the matrix elements for $\sigma$ transitions are in the ratio of $1:\sqrt{3}$, resulting in Eq. (68) with $p_2/p_1=\sqrt{3}$. The familiar form of $-\frac{\alpha}{2}\sin A$ is not reproduced for larger J and J'. It is curious that for J or J'=$\frac{1}{2}$ or 3/2 the analysis holds for $\pi$ transitions, but not for $\sigma$ transitions. If a circularly polarized light pulse enters such a medium the result may be that the system will be unstable against the formation of linearly polarized $2\pi$ h.s. pulses.

For large J, J', the results degenerate into the classically derived formulae. Specifically for large J=J'$\pm$1 in the presence of $\pi$ transitions, or for large J=J' and in the presence of $\sigma$ transitions, Eq. (69) results; and for large J=J'$\pm$1 in the presence of $\sigma$ transitions, or for J=J' in the presence of $\pi$ transitions, Eq. (70) results. It must be emphasized that along with J must also be included the effect of hyperfine interactions, unless the resultant hyperfine splitting is characterized by an energy $\ll \hbar/\tau$. If a magnetic or electric field is applied to remove the degeneracies in the above problem, the results are unchanged providing that the frequency splitting of the degeneracies is small compared to the inverse pulse width $\tau^{-1}$ both and the inverse Doppler linewidth $\sim T_2^{*\,-1}$.

## IV. EFFECTS OF RELAXATION TIMES ON PULSE TRANSMISSION

The effects of weak damping upon the plane wave $2\pi$ h.s. pulse are now assessed for the condition $\tau/T_2' \ll 1$. It will be shown that the pulse energy decays linearly with distance, the pulse area deviates to a value slightly below $2\pi$, and the pulse delay time can deviate considerably from the previously derived value.

### Pulse Energy Damping

With the pulse energy per $cm^2$ defined by Eq. (41), integration of Eq. (22), and use of Eqs. (24), (25), and (26), leads to the resulting expression of energy conservation:

$$\frac{dJ}{dz} = -\int_{-\infty}^{\infty} [W(\Delta\omega,z,t_o) - W_o(\Delta\omega)]g(\Delta\omega)d\Delta\omega$$

$$-\int_{-\infty}^{t_o} dt \int_{-\infty}^{+\infty} \frac{[W(\Delta\omega,z,t) - W_o(\Delta\omega)]}{T_1} g(\Delta\omega)d(\Delta\omega). \qquad (72)$$

The time $t_o$ is defined after the light pulse has decayed to zero. The first term represents the residual energy stored in the two-level system; whereas the second term represents the energy that was taken from the light pulse and temporarily stored in the system, but which has decayed by a $T_1$ relaxation process (e.g. spontaneous emission).

To assess the pulse energy decay behaviour with $T_1$ and $T_2'$ finite, it is convenient to consider the modified form of $u^2+v^2+\frac{\kappa^2 W^2}{\omega^2} = W_o^2$, a consequence of Eq. (18), when relaxation processes are introduced. Upon multiplying Eqs. (24), (25), and (26) by u, v, and W, respectively, adding and performing a time integration, then

$$\frac{\kappa^2}{\omega}W^2(\Delta\omega,z,t) + u^2(\Delta\omega,z,t) + v^2(\Delta\omega,z,t)$$

$$= \frac{\kappa^2}{\omega}W_o^2 - 2\int_{-\infty}^{t} dt' \frac{[u^2(\Delta\omega,z,t') + v^2(\Delta\omega,z,t')]}{T_2'}$$

$$- 2\left(\frac{\kappa^2}{\omega^2}\right)\int_{-\infty}^{t} dt' \frac{W(\Delta\omega,z,t')[W(\Delta\omega,z,t') - W_o]}{T_1}. \qquad (73)$$

At $t = \infty$, u, v, and W will have relaxed by damping to their equilibrium values u=v=0 and $W=W_o$, respectively, which they had at $t = -\infty$. Therefore, Eq. (73) implies that

$$\int_{-\infty}^{\infty} dt' \left\{ \frac{u^2(\Delta\omega,z,t')+v^2(\Delta\omega,z,t')}{T_2'} + \frac{\kappa^2}{\omega^2} \frac{W(\Delta\omega,z,t')[W(\Delta\omega,z,t') - W_o]}{T_1} \right\} = 0. \qquad (74)$$

In Eq. (72), we may choose $t_o$ anytime after the pulse has subsided at a given position z. The dominant contribution in Eq. (72) is then the integral for $t_o \gg T_1$. However, since $W(t_o) - W_o \sim \exp(-t/T_1)$, the sum of the two integrals must be independent of $t_o$. Having chosen $t_o \gg T_1$, only the second integral need be considered. Using Eq. (74), Eq. (72) reduces to

$$\frac{dT}{dz} = - \frac{2}{N\hbar\omega}\int_{-\infty}^{+\infty} dt \int_{\infty}^{-\infty} g(\Delta\omega) d\Delta\omega \left\{ \frac{[W(\Delta\omega,z,t)-W_o]^2}{T_1} \right.$$

$$\left. + \left(\frac{\omega^2}{\kappa^2}\right) \frac{[u(\Delta\omega,z,t)^2 + v(\Delta\omega,z,t)^2]}{T_2'} \right\}. \qquad (75)$$

This formula is independent of the approximations $\tau \ll T_1, T_2'$, and is true for pulses which are not necessarily $2\pi$ h.s. pulses. Upon traveling through the slightly lossy medium, an electric field pulse which deviates

from the ideal $2\pi$ h.s. form, only because $T_1$ and $T_2'$ are finite, will induce a polarization for which the above formula can be evaluated to first order in $\tau/T_2'$. We may for example write $u = u(s)\sin(\varphi/2) + \Delta u$, where $u(s)$ is the coefficient of $\sin(\varphi/2)$ in Eq. (52), and $\Delta u$ is a small correction of order $\tau/T_2'$. The integration over $u^2$ in Eq. (75) will yield terms at least of the order $(\tau/T_2')^2$ from the integrand terms $(\Delta u)u(s)\sin(\varphi/2)/T_2'$ and $(\Delta u)^2$. Since only the first order correction is desired these may be dropped and we may replace u in Eq. (75) by $u(s)\sin\varphi/2$. Similarly v and W may be replaced by the zero order solutions given by Eqs. (53) and (54). Then after performing the time integrations in Eq. (75) we obtain

$$\frac{dT}{dz} = -4N\hbar\omega\tau\left[\int_{-\infty}^{\infty}\frac{g(\Delta\omega)d(\Delta\omega)}{1+\Delta\omega^2\tau^2} + \left(\frac{2}{3}\right)\left(\frac{1}{T_1} - \frac{1}{T_2'}\right)\int_{-\infty}^{\infty}\frac{g(\Delta\omega)d(\Delta\omega)}{(1+\Delta\omega^2\tau^2)^2}\right]. \tag{76}$$

For the extremely narrow line case, the spectral distribution may be defined as a delta function ($\frac{1}{T_2^*} = \infty$, no inhomogeneous broadening) $g(\Delta\omega) = \delta(\Delta\omega)$, and Eq. (76) becomes

$$\frac{dT}{dz} = -\frac{4N\hbar\omega\tau}{3}\left[\frac{1}{T_2'} + \frac{2}{T_1}\right] = -\frac{8N\hbar\omega\eta c}{3\pi\kappa^2}\left(\frac{1}{T_2'} + \frac{2}{T_1}\right)\frac{1}{T}, \tag{77}$$

since

$$T \approx 2\eta c/(\pi\kappa^2\tau) \tag{78}$$

by letting $\dot{C}(t) = \frac{2}{\kappa\tau}\mathrm{sech}(\frac{t}{\tau})$ in Eq. (41). For the inhomogeneous broad line case, $g(\Delta\omega)$ is constant over the region of excitation and

$$\frac{dT}{dz} = -\left(\frac{4\pi}{3}\right) N\hbar\omega g(0)\left(\frac{1}{T_1} + \frac{2}{T_2'}\right). \tag{79}$$

The pulse energy loss rate expressed by Eq. (79) is plausibly expressed as the product of the number of quanta $N\hbar\omega T_2^*/\tau$ absorbed from the pulse and given back to it, the damping rate $1/T_1 + 2/T_2'$, and the time $\tau$. We must keep in mind that Eqs. (77) and (79) are valid only for $\tau \ll T_2', T_1$.

If several $2\pi$ h.s. pulses are propagating through a slightly damped medium, the above formulae apply to each of the individual pulses. Situations may arise in which the number of $2\pi$ h.s. pulses is so large, that the additive effect of preceeding pulses cannot be ignored. Imagine a train of $n2\pi$ h.s. pulses, and suppose that $T_1$ is much longer than the total time required for the train of pulses to pass a point z. $T_2'$, however, still is required to be much longer than an individual pulse width, but no restrictions need necessarily be placed upon the time span of the total train as compared with $T_2'$.

Under such conditions, the first several of the train of $2\pi$ h.s. pulses lose energy as dictated by Eq. (76), whereas another $2\pi$ h.s. pulse loses energy as dictated by an equation similar to Eq. (76), but with $g(\Delta\omega)$ appropriately modified to take into account the change in spectral population due to the action of all preceeding pulses. The first pulses in the train each therefore lose more energy than the trailing pulses. Since the velocity of a $2\pi$ h.s. pulse increases with its energy, and also increases as $g(\Delta\omega)$ decreases (Eq. (56)), the trailing pulses will tend to overtake the first pulses in the train. How pulse splitting effects, illustrated in Fig. (7), counteracts this tendency for pulses of similar initial time widths to converge is not yet known.

Effect of Relaxation Upon Pulse Delay

The effect of damping upon the pulse delay time can be calculated on the basis of assumptions used for pulse energy damping. Define the delay time as $t_d = \int_o^z \frac{dz}{V(z)}$, replacing z in Eq. (42), where we assume $V = V(z)$ is a slowly varying function of z; and let $\frac{1}{V(z)} = \frac{\alpha\tau(z)}{2} = \frac{dt_d}{dz}$ for a $2\pi$ h.s. pulse. Therefore,

using T expressed by Eq. (78), and $\frac{dT}{dz} = \frac{dT}{dt_d}\frac{1}{V(z)}$ together with Eq. (79) and the definition of $\alpha$ (Eq. (36)), we obtain

$$\frac{dT}{dt_d} = -\frac{1}{T_e}T, \tag{80}$$

where $\frac{1}{T_e} = (\frac{4}{3})\left(\frac{1}{T_2'} + \frac{1}{2T_1}\right)$ and $\tau(z) \ll T_e$. The form of Eq. (80) implies that it is the result of a first order correction perturbation evaluation. For a given delay time $t_d$, Eq. (80) states that $T(t_d) = T(t_d=0)e^{-t_d/T_e}$, where the $2\pi$ h.s. output pulse energy is evaluated at different distances z, corresponding to a given delay time $t_d$. If we define $t_d = T$ when z = L, the length of the medium, and if we assume $t_d=0$ at z=0, then

$$L = \frac{2}{\alpha}\int_0^T (\frac{1}{\tau(t_d)})dt_d. \tag{81}$$

Since $\tau T$ is constant from Eq. (78), then from Eq. (80), $\tau(t_d) = \tau_o e^{t_d/T_e}$, where $\tau_o$ is the input pulse width. Finally, Eq. (81) expresses

$$T = -T_e \log\left(1 - \frac{\alpha L \tau_o}{2T_e}\right) \tag{82}$$

as the total delay time. From Eq. (81), the final pulse width (z=L) becomes $\tau(L) = \tau_o/(1 - \alpha L\tau_o/2T_e)$. The net delay may be therefore written as

$$T = T_e \log(\tau/\tau_o). \tag{83}$$

From the limitation that $\tau < T_e$, the maximum expected delay time for parallel beam conditions may be estimated to be about $T_e\log(T_e/\tau_o)$.

Stable Pulse Propagation Solution with Damping

Loss of pulse energy in a passive homogeneously broadened medium caused by $T_2'$ and $T_1$ damping can be compensated by focusing the light beam down the rod. Formally this is accomplished by adding a term $\sigma\mathcal{E}$ to the right side of Eq. (43), which will then cancel out an expected loss term from the integral over $v(\Delta\omega,z,t)$. The constant $\sigma$ is ideally determined by parameters consistent with the pulse solutions to the optical Bloch equations. In practice deviations of the focusing parameter from

$\sigma$ will occur over sufficiently long distances z, so that the balance provided by $\sigma\mathcal{E}$ is actually unstable, and the pulse will eventually decrease or increase because of the instability. Assuming the ideal balance condition reasonably applicable to a short sample rod, we consider a soluble case where the sample is purely homogeneously broadened by $1/T_2'$ (with $1/T_2^* = 0$ and $1/T_1 = 0$), and optical excitation is at exact resonance.

Solutions which satisfy Eq. (43) (with $\sigma\mathcal{E}$ added to it) and Eqs. (24), (25), and (26) are found on the basis that the stable pulse with area $\theta = 2\pi$ is expressed by

$$\mathcal{E}(z,t) = \frac{2}{\kappa\tau}\sin[\varphi(z,t)] = \frac{2}{\kappa\tau}\operatorname{sech}\frac{1}{\tau}(t - z/V_d), \tag{84}$$

and

$$\frac{\partial\mathcal{E}}{\partial z} = -(1/V_d)\frac{\partial\mathcal{E}}{\partial t}. \tag{85}$$

The inverse pulse velocity is now

$$1/V_d = \frac{\eta}{c} + \frac{2\pi\omega\kappa N p\tau\,\tau_d}{\eta c} \tag{86}$$

where $\tau_d$ is given in terms of the actual pulse width $\tau$ by:

$$\tau_d = \tau/\left(1 + \frac{4}{3}\frac{\tau}{T_2'} + \frac{\tau^2}{3T_2'^2}\right), \tag{87}$$

and the focusing parameter is given by $\sigma = (1/V_d - \eta/c)/3T_2'$. The Bloch equation solutions on resonance are

$$u = 0$$

$$v = [N p\sin\varphi + \frac{2\tau}{3T_2'}\, N p\sin(\varphi/2)](\tau_d/\tau), \tag{88}$$

and $$W = -\frac{\kappa}{\omega}\left[\cos\varphi + \frac{4\tau}{3T_2'}\cos\frac{\varphi}{2} + \frac{\tau^2}{3T_2'^2}\right](\tau_d/\tau), \tag{89}$$

where $\varphi(t,z)$ is given by Eq. (30).

These solutions apply as well to the dynamics of the polarization in a cavity, as given by J. Bloom[6] relative to a radiation damping problem in nuclear induction. We have not solved the above case when the line is also inhomogeneously broadened ($T_2^*$ finite).

Effect of Relaxation Upon Pulse Area

In the limit that $T_2'$ and $T_1$ are very short compared to pulse width $\tau$, ordinary rate equations would apply to give a "hole burning" or nonlinear saturation solution to the pulse propagation problem. The intermediate case of $\tau \sim T_2'$ has so far been analytically intractable, but an explicit small correction to the quasi-steady state hyperbolic secant solution can be made in the case of $\tau < T_2', T_1$ by a slight alteration of the $2\pi$ condition. The "$2\pi$" area condition for the h.s. pulse is altered to first order and is diminished slightly to the value (see Appendix B)

$$A \approx 2\pi(1 - \tau/T_2'). \tag{90}$$

Appendix B presents a generalized form of the area theorem which includes damping. It is not valid simply to replace $g(0)$ by $T_2'/\pi$ in $\alpha$, which occurs in the area theorem expressed by Eq. (36), if homogeneous broadening is the sole cause of the line width.

## V. EFFECT OF DOPPLER VELOCITY SHIFTS IN GASES

For gaseous particles, which at rest would be at exact electric dipole resonance with the applied optical frequency $\omega$, a Doppler frequency shift

$$\Delta\omega = \omega_o - \omega = kv_z \tag{91}$$

is present for those dipoles moving with velocity $v_z$ along the propagation direction z of the light pulse. In this section it is shown that most of the properties of self-induced transparency which have been discussed will apply to resonant gases, except that the pulse velocity and area undergo a transformation when the spectral line is excited off-resonance. This transformation constitutes the principle difference between the resonance response of dipoles fixed in a solid (e.g. ruby[10]) and dipoles moving in a gas (e.g. sulfur hexafluoride[12]). In the gas the dipoles can move in the z direction through a slowly moving pulse envelope $\mathcal{E}(z,t)$ (of low pulse velocity V) in a time comparable to the pulse width $\tau$.

Consider an atom which is originally at position $z_o$ at t=0, which interacts with the electric field $E(z_o+v_zt,t)=\mathcal{E}(z_o+v_zt,t)\exp[i(\omega-kv_z)t-kz_o]$, where $z = z_o + v_zt$ and the phase term $\phi(z)$ in Eq. (19) is absorbed into the modulus $\mathcal{E}$, making it a potentially complex quantity. Relaxation by collision is neglected by assuming that $\tau$ is short compared to the time between collisions. We first show that the motion of the dipoles has negligible effect in the evaluation of $\mathcal{E}$ when the spectral line is excited at the peak of its resonance. For an inhomogeneously broadened Doppler spectral frequency width greater than the inverse pulse width $1/\tau$, only those atoms are excited which have a range of Doppler velocities extending from $v_z=0$ to $v_z \sim \pm \frac{c}{\omega\tau}$. Therefore, the dipoles can move at most through a distance $v_z\tau \cong \lambda$ during a pulse width time $\tau$. Since the spatial extension along the

z direction of a transparency type pulse is approximately $\alpha^{-1}$, and because the condition $\alpha^{-1} \gg \lambda$ holds in order to avoid strong coherent backscattering, the small displacement of atoms through a distance $\lambda$ will not impose any significant variation upon the field modulus $\mathcal{E}(z_o+V_z t,t)$.

The Hamiltonian for a particle dipole of the gaseous system should be written as

$$\mathcal{H} = \mathcal{H}_o - \underset{\sim}{p}_o \cdot \underset{\sim}{E}(z,t) - \frac{\hbar^2}{2m}\nabla^2, \tag{92}$$

where the kinetic energy operator of the particle of mass m is added to the static Hamiltonian, Eq. (3); and we define $z = z_o + v_z t$, $\underset{\sim}{r}$ the center of particle mass m, $m\underset{\sim}{v} = \hbar \underset{\sim}{k}_m$, and $\underset{\sim}{v}$ the particle vector velocity. Negligible particle recoil effects may be ignored, and the dipole two level wave function $\psi$ is therefore separable from the particle wave function. The latter is assigned a kinetic phase factor $\exp i(\underset{\sim}{k}_m \cdot \underset{\sim}{r} - \frac{\hbar k^2 t}{2m})$, but this factor has no effect upon the optical pulse resonance behaviour of the two level system.

Now define an observer at rest with respect to the dipole in a Galilean frame of reference moving with velocity $V_g$, and write $z=z_\ell=z_g+V_g t$, where $z_\ell$ and $z_g$ are respectively laboratory and Galilean coordinates, and $V_g=v_z$ for the single particle. The laboratory Hamiltonian Eq. (92) will satisfy the time dependent Schroedinger equation when the respective laboratory and Galilean frame wave function $\psi_\ell$ and $\psi_g$ are related by the transformation

$$\frac{\partial \psi_\ell(z,t)}{\partial t} = \frac{\partial \psi_g(z_g,t)}{\partial t} - V_g \frac{\partial \psi_g(z_g,t)}{\partial z_g} . \tag{93}$$

The density matrices $\rho_\ell(z,t)$ and $\rho_g(z_g,t)$ are related to one another in the same way. To evaluate the spatial derivative in Eq. (93), let us inspect the electric fields $E(z_g,t)$ and $E(z_g+\Delta z,t)$ which interact respectively with two dipoles having the same Doppler frequency shift $\Delta\omega$ or velocity $V_g$, but are separated by a small distance $\Delta z$. It was pointed out earlier that the greatest distance an excited dipole would travel during the pulse time $\tau$ is of the order of $\lambda$, so that the separation $\Delta z$ under consideration is governed by the relation $\lambda \sim \Delta z \ll \alpha^{-1}$. One sees therefore that any variation with $\Delta z$ of the field modulus $\mathcal{E}(z_g,t)$ experienced by dipoles, moving toward or away from position $z_g$ at which the pulse is defined, may be neglected. The only difference in the value of the electric field at the positions separated by $\Delta z$ is imposed by the phase difference of the light taking place over a wave length. Therefore, with the condition that $\alpha\lambda \ll 1$, the relationshp $E(z_g+\Delta z,t) = E(z_g,t-\Delta z/c)$ holds, which signifies that the two dipoles have experienced the same history of excitation by the field except for a time delay $\Delta z/c$. Therefore the relation

$$\psi_g(z_g + \Delta z,t) = \psi_g(z_g,t - \frac{\Delta z}{c}) \tag{94}$$

will apply, and a Taylor expansion of both sides of Eq. (94) yields

$$\frac{\partial \psi_g(z_g,t)}{\partial z_g} = -\frac{1}{c}\frac{\partial \psi_g(z_g,t)}{\partial t} \tag{95}$$

to order $\alpha\lambda \ll 1$. Use of Eq. (95) in Eq. (93) allows the time dependent Schroedinger equation to be written as

$i\hbar\dot{\psi}_\ell(z,t)=i\hbar(1+V_g/c)\dot{\psi}_g(z_g,t)=\mathcal{H}_\ell(z,t)\psi_\ell(z,t)=(1+V_g/c)\mathcal{H}_g(z_g,t)\psi_g(z_g,t)$

where $\mathcal{H}_\ell(z,t)$ is given by Eq. (3) with $\omega_o = \omega_o$. With $\psi_\ell(z,t) = \psi_g(z_g,t)$, therefore

$$i\hbar\dot{\psi}_\ell(z,t) = H_\ell(z,t)\ \psi_\ell(z,t) \tag{96}$$

where $\mathcal{H}_\ell(z,t) = (1 + V_g/c)\mathcal{H}_g(z_g,t)$. The small term in $V_g/c \ll 1$ may be dropped as a factor of the $\underset{\sim}{p} \cdot \underset{\sim}{E}$ term in the Galilean Hamiltonian $\mathcal{H}_g(z_g,t)$, so that $H_\ell(z,t)$ is given by Eq. (3) with $\omega_o = \omega(1+V_g/c)$. Subsequent steps in the analysis following Eq. (3) will therefore include in a natural way the inhomogeneous broadening contributed by the Doppler frequency shift $\Delta\omega = kV_g$, which follows by virture of the term $-\frac{V_g}{c}\mathcal{H}_o$ introduced in Eq. (96).

The spectral integration in Eq. (21) applies with $g(\Delta\omega)$ now to be defined as the normalized Maxwell-Boltzman velocity distribution function, and $v_z = V_g$ pertains to any one of the velocities in the Doppler spectrum. The electric field E acts at position z upon dipoles with a range of velocities $v_z$ which started from different positions $z_g$ at t = 0. If the phase factor $\exp i[(\omega-kv_z)t - kz_g]$ is chosen in Eq. (21), integration over a distribution of positions $z_g$ would be cancelled by integration over velocities $v_z$ contained in this phase factor. This property of cancellation is expressed by retaining the equivalent phase factor $\exp i(\omega t-kz)$, where z is a constant of the integration. However, the polarization u + iv still remains as a function of $\Delta\omega = kv_z$, to be integrated over $g(\Delta\omega)$, now defined as the Maxwell-Boltzman distribution of velocities. The area theorem given by Eq. (36) remains unaffected by Doppler frequency shifts, or by any effects these may have on the pulse shapes themselves. The area theorem derives from those dipoles having zero velocity ($\Delta\omega=0$) in the Boltzman distribution, and it is only these dipoles which contribute to the polarization $v(0,z,t)$.

Although the analysis above is not generally applicable to the case where $g(\Delta\omega)$ is asymmetrically excited off-resonance, it can be applied to the analysis of the $2\pi$ h.s. pulse solution expressed earlier by Eq. (42). In this case the conditions given by Eq. (94) and (95) are again valid if the problem is analyzed in a reference frame moving with a velocity $V_g$ chosen to coincide with the velocity of dipoles at exact resonance with the applied pulse. Relative to this moving frame the pulse may be considered to excite a sufficiently small band of Doppler broadened frequencies so that $|V_g - v_z|\tau \ll \alpha^{-1}$, which is a consequence of $\alpha^{-1} \gg \lambda$. Let the peak of the distribution $g(\Delta\omega)$ be excited off-resonance by an amount $\Omega$. The resonant dipoles move with an average laboratory velocity,

$$V_g = c\Omega/\omega. \tag{97}$$

The analysis of the off-resonance excitation of an inhomogeneous Doppler broadened system, which leads to a $2\pi$ h.s. solution of the form of Eq. (42), now requires that $v_z$ be replaced by $v_z + V_g$ in Eq. (91).

The pulse velocity $V_{p\ell}$ in the laboratory frame is now defined as

$$V_{p\ell} = V_{pg} + V_g, \tag{98}$$

where $V_{pg}$ is the pulse velocity in the Galilean frame. The $2\pi$ h.s. field pulse in the Galilean frame is expressed as

$$\mathcal{E}(z_g,t) = \left(\frac{2}{\kappa\tau_g}\right)\operatorname{sech}\left[\frac{1}{\tau_g}\,(t - z_g/V_{pg})\right], \tag{99}$$

with $\tau_g$ defined as the Galilean frame pulse width, and $V_{pg} = 2/(\alpha\tau_g)$. The observed pulse in the laboratory frame is obtained from Eq. (99) by substituting $z_g = z - V_g t$ so that

$$\mathcal{E}(z,t) = \left(\frac{2V_{pg}}{\kappa\tau_\ell V_{p\ell}}\right)\operatorname{sech}\left[\frac{1}{\tau_\ell}\left(t - \frac{z}{V_{p\ell}}\right)\right], \tag{100}$$

$\tau_\ell = \tau_g V_{pg}/V_{p\ell}$ is the laboratory pulse width, and $V_{p\ell} \approx 2/(\alpha\tau_\ell)$.

A curious property arises if we imagine that the pulse given by Eq. (100) excites the gas. Let the gas be given a real flow velocity $V_g$ in the negative z direction so that $V_{p\ell} = V_{pg} - |V_g|$ passes through zero and $V_{p\ell}$ becomes negative, as seen from Eq. (98). At $V_{p\ell}=0$ the pulse will momentarily stop, suspended in space, and acquire an "infinite width". As $V_{p\ell}$ becomes negative the pulse moves backwards toward the entrance window from which it came.

At $t = \infty$ the laboratory frame pulse area is $A_\ell(\infty) = 2\pi(V_{pg}/V_{p\ell})$, which is not equal to $A_g(\infty) = 2\pi$ for the pulse in the Galilean frame. However, the tipping angles $\varphi$ for the polarization $\underset{\sim}{P}(0,z,t)$ are the same in both frames. The tipping angle is given by the pulse area in the frame moving at the velocity of exactly resonant atoms

$$\theta = \kappa\int_{-\infty}^{+\infty} \mathcal{E}(z_g,t)dt = 2\pi$$

Equally well we may find $\theta$ in the laboratory frame by calculating the time integral of the electric field modulus at the site of a moving atom:

$$\theta = \kappa\int_{-\infty}^{+\infty} \mathcal{E}(z_L+V_g t,t)dt = \int_{-\infty}^{+\infty} \frac{2V_{pg}}{\tau_\ell V_{p\ell}} \operatorname{sech}\frac{1}{\tau_\ell}\left(t - \frac{z}{V_{p\ell}} - \frac{V_g t}{V_{p\ell}}\right) dt.$$

This quantity is equal to $(1 - V_g/V_{pL})^{-1}A_\ell(\infty)$, which, in view of Eq. (98), reduces to $\theta = 2\pi$. The addition $k' = \partial\phi/\partial z$ to the propagation vector is unchanged by the transformation.

## VI. AMPLIFIED $\pi$ PULSE SOLUTION WITH NO DAMPING

A number of authors[23] have investigated the problem of a propagating amplified light pulse. Hopf and Scully[24], in particular, have treated the problem for an inhomogeneously broadened line. An analytic description of a continually amplified pulse is difficult to obtain, but we can present one on the basis that the pulse leading edge is nearly infinitely steep, and that it travels essentially at velocity $c/\eta$. As previously noted the area theorem (Eq. (38)) states that a pulse in an amplifying two level system evolves toward a $\pi$ pulse. Although the area is fixed at $\pi$ the pulse width $\tau$ shortens with increasing distance as long as $\tau \gg T_2^*$, where $T_2^*$ is the inverse inhomogeneous line width. The pulse energy therefore must increase with z at a rate which would slacken as the pulse shortens to the point where $\tau \sim T_2^*$. The pulse shape would correspondingly undergo a radical change. We present a solution for the pulse shape in the range where $\tau \gg T_2^*$ -- a pulse function which is essentially invariant for all z and satisfies the combined Maxwell and optical Bloch equations.

If the leading edge of the pulse is defined analytically it would be impossible to obtain an overall pulse function which would describe both the linearly amplified leading edge, governed by the power gain factor $\sim \exp(\alpha)$, and the main profile of the pulse of width $\tau$ which follows at a lesser gain. The smaller gain for the lagging portion of the pulse is expressed by the factor F in Eq. (40), which is less than unity. The sharp front of the pulse will be given a finite rise time short compared to $\tau$, but comparable to or long compared to $T_2^*$. These restrictions on the rise time will allow the pulse edge to be described as almost infinitely sharp. The pulse peak at the leading edge will be given an amplification $\sim \exp(\alpha z/2)$, while the $\pi$ area of the declining pulse envelope which follows is maintained by requiring that its pulse width decrease as $\sim \exp(-\alpha z/2)$. The resulting pulse will have an energy gain

$\sim \exp(\alpha z/2)$. The sharp edge on the pulse will be formed and will persist by the action of saturable filters placed within the amplifying medium in order to stabilize it.

A pulse which satisfies the above limiting behaviour is the "half-hyperbolic secant solution", where the leading edge travels along the line $t = \eta z/c$:

$$\mathcal{E}(z,t) = \begin{cases} 0 \text{ for } t - \eta z/c < 0 \\ \frac{2}{\kappa\tau(z)}\operatorname{sech}\left\{\frac{1}{\tau(z)}\left(t - \frac{\eta z}{c}\right)\right\} \text{ for } t - \frac{\eta z}{c} > 0, \end{cases} \tag{101}$$

and the inverse pulse width is given by

$$\tau^{-1}(z) = \tau^{-1}(z=0)\exp\left(\frac{\alpha z}{2}\right). \tag{102}$$

The corresponding solutions to Eqs. (24), (25), and (26) are now for $t > \eta z/c$ respectively

$$u = Np\, f^2[-2\Delta\omega\tau\cos(\Delta\omega t) - 4(\Delta\omega\tau)^2\sin(\Delta\omega t)\tanh(t/\tau) + 2(\Delta\omega\tau)^3\cos(\Delta\omega t) - (\Delta\omega\tau)^3\kappa\mathcal{E} + \Delta\omega\tau\kappa\mathcal{E}], \tag{103}$$

$$v = Npf^2[1-\Delta\omega^2\tau^2)\sin\varphi - 4\Delta\omega^2\tau^2\tanh(t/\tau)\cos\Delta\omega t - 2\Delta\omega^3\tau^3\sin\Delta\omega t + 2\Delta\omega\tau\cos\varphi\sin\Delta\omega t], \tag{104}$$

$$\frac{\kappa}{\omega}W = Npf^2\,[-\Delta\omega^2\tau^2(1-\Delta\omega^2\tau^2) - (1-\Delta\omega^2\tau^2)\cos\varphi + 2\Delta\omega^2\tau^2\kappa\mathcal{E}\cos\Delta\omega t + 2\Delta\omega\tau \sin\Delta\omega t \sin\varphi] \tag{105}$$

if t above is replaced by $t-\eta z/c$, $f = f(\Delta\omega)$ is given by Eq. (51), and $\varphi = 4\tan^{-1}(e^{t/\tau})$. For a Lorentzian line shape, $g(\Delta\omega) = \dfrac{(T_2^*/\pi)}{1+\Delta\omega^2 T_2^{*2}}$, and therefore

$$\int_{-\infty}^{\infty} g(\Delta\omega)v(\Delta\omega)\dot{a}(\Delta\omega) = -\frac{1}{2}NpT_2^*\kappa\mathcal{E}\left(1 - \frac{t}{\tau}\tanh\frac{t}{\tau}\right) + \frac{2Np\ T_2^*}{\tau}\exp\left(-t/T_2^*\right)\Phi$$

+ terms of order $T_2^{*2}/\tau^2$. (106)

It can now be verified that Eq. (22) is satisfied, except for the negligible last two terms in Eq. (106) above. Fig. (8) shows a plot of the change with distance of a pulse shape injected at z = 0. It is assumed that a saturable filter immediately absorbs enough of the leading edge of the pulse to form a sharp leading edge which begins to grow; therefore, the pulse evolves into a half-hyperbolic secant $\pi$ pulse shape. The beginning oscillations of the pulse are drawn in qualitatively. Only after the pulse leading sharp edge develops and the oscillations subside does the amplified half $2\pi$ h.s. pulse conform to the analysis given above.

## VII. EFFECT OF TRANSPARENCY ON PHOTON ECHOES

The area theorem given by Eq. (38) specifies that a given input area $\theta_o$ evolves into a final area $\theta(z)$ at position z, but it cannot predict a photon echo[7] since the theorem does not give any information about pulse shape. Nevertheless, in an extended medium some important properties of the photon echo can be deduced from the theorem; namely, it can describe some aspects of the echo pulse area and support the justification that the echo peak will not necessarily occur at times $2\tau_s$ at the output position z, where $\tau_s$ is the separation time between input pulses at z = 0. Suppose a $\pi/2$ - $\pi$ pulse sequence, corresponding to input pulses $\theta_1(0)$ and $\theta_2(0)$, is injected at z = 0, where $\tau_s$ is sufficiently large so that the two pulses do not overlap. The area theorem requires that the $\pi/2$ pulse will decay to zero for $z \gtrsim \alpha^{-1}$. This condition applied in the gaseous $SF_6$ photon

echo experiment of Patel and Slusher[25]. Since the total injected area is $\theta_1(0) + \theta_2(0) = 3\pi/2$, the final area in the output becomes $2\pi = \theta_2(z) + \theta_e(z)$, where $\theta_e(z)$ is the sum of areas of possible multiple echoes following the $\theta_2(z)$ pulse. The most important first echo following the $\theta_2(z)$ pulse will tend to be delayed and will occur at a time $> 2\tau_s$ because the aggregate of all pulses will broaden as the sum of pulse areas increase together toward $2\pi$. Of course in the output the predominant echo following the $\theta_2(z)$ pulse may have an amplitude greater than the first $\theta_1(z)$ pulse since the latter tends to diminish toward zero amplitude.

For any sample thickness, the dependence of the echo area $\theta_e$ is obtained from Eq. (38) as

$$\theta_e(z) = 2\tan^{-1}\left\{\left[\tan\tfrac{1}{2}(\theta_1(0) + \theta_2(0))\right]\exp(-\frac{\alpha z}{2})\right\} - \theta_1(z) - \theta_2(z) \qquad (107)$$

where

$$\theta_1(z) = 2\tan^{-1}\left\{\left[\tan\tfrac{1}{2}\theta_1(0)\right]\exp(-\frac{\alpha z}{2})\right\}$$

is the solution of $\dfrac{d\theta_1(z)}{dz} = -(\alpha/2)\sin\theta_1(z)$; and

$$\theta_2(z) = 2\tan^{-1}\left\{\left[\tan\tfrac{1}{2}\theta_2(0)\right]\exp\left[\int_0^z(-\frac{\alpha}{2}\cos\theta_1(z)dz\right]\right\}, \qquad (108)$$

is the solution of $\dfrac{d\theta_2(z)}{dz} = -\left[\dfrac{\alpha}{2}\cos\theta_1(z)\right]\sin\theta_2(z)$. The effective "$\alpha$" for the second $\theta_2$ pulse is given as $\alpha\cos\theta_1(z)$, which is proportional to the number of on-resonance dipoles that remain in the ground state after the $\theta_1$ pulse has subsided. Therefore Eq. (108) gives

$\theta_2(z) = 2\tan^{-1}\left\{\frac{\sin\theta_1(z)}{\sin\theta_1(0)}\tan\left(\frac{\theta_2(0)}{2}\right)\right\}$. For small z, the small echo area is given by $\theta_e(z) = \frac{\alpha}{2}\sin\theta_1(0)[1-\cos\theta_2(0)]z$, which is a maximum for $\theta_1(0) = 90^\circ$ and $\theta_2(0) = 180^\circ$, the same optimum condition which applies for obtaining a maximum spin echo[8] signal.

## VIII. EXPERIMENTAL RESULTS

The preceding analysis is based upon two important assumptions: (1) the propagating light pulse contains no frequency modulation, and (2) the pulse is described in terms of a plane wave. Computer calculations contain these assumptions and reveal that a $2\pi$ h.s. pulse continues to propagate. Yet the basic character of such a pulse shows up in actual experiment where the pulse input is undoubtedly frequency modulated, and the pulse is not in the form of a plane wave. The observed self-induced transparency pulse appears to stabilize against frequency modulation, and the pulse persists in spite of non-plane wave conditions. In the previous analysis small deviations from ideal assumptions do introduce small losses, but the deviation which is most serious is any departure from the plane wave condition. Transverse mode effects (as introduced by Eqs. (64) and (65)) or diffraction effects cause strong deviations which are not completely understood. Transverse deviations in beam behaviour will grow seriously with path distances exceeding a few Beer absorption lengths.

The purpose of our experiments with ruby is to check how far the experimental results conform to the phenomenological predictions of the plane wave transparency model, and to set forth those observed pulse characteristics which are in disagreement with the predictions. Fig. (9) indicates a particular experimental arrangement for measuring pulse delays, but applies as well to a number of other measurements. A Q-switched liquid nitrogen-cooled laser oscillator is followed by a ruby laser

amplifier which selects and amplifies the plane polarized $\bar{E}(2E) \leftrightarrow {}^4A_2(\pm 3/2)$ output laser line, as indicated in the energy level diagram of of Fig. (10a). The laser amplifier scheme is shown in Fig. (11). By thermal tuning, the passive target ruby sample cooled at liquid helium temperature to reduce phonon relaxation presents the ${}^4A_2(\pm\frac{1}{2}) \leftrightarrow \bar{E}(2E)$ transition which is tuned to the driving laser pulse. The target sample (0.05% $Cr^{+3}$ in $Al_2O_3$) is $0^\circ$ c axis oriented, of $\frac{1}{2}$ in. diameter, and 2 and 3/4 in. length along the z axis. The input pulse to the amplifier was of multimode character longitudinally, but was of a selected single transverse mode. Defocusing of the transverse beam profile by abberations in the amplifier ruby rod was compensated by converging the amplifier input so that when the amplifier output was recollimated (~ f - 25 system) an image of the amplifier rod was formed near the sample. Peak outputs between 1 and 10 megawatts were available.

For non-linear transmission measurements of deviations from Beer's law, the simplest possible arrangement of source, sample, and detector was used. Corning glass filters, checked for linearity, were put behind and in front of the sample. The output light was photographed with Polaroid Type 47 film at the image plane of the exit end of the sample replacing the mirror in Fig. (9).

The simplest demonstration of non-linear transmission is to move attenuators from behind the sample to in front of the sample, while keeping the total filter attenuation constant. If the sample responds linearly, then the placement of attenuators would make no difference in the total transmission. If the sample transmits non-linearly, then more energy should be transmitted with attenuators behind the sample. Figs. (12a) and (12b) show reproductions of the photographed transmitted output,

with the input and output attenuations indicated. Fig. (12a) resulted from use of a multi-transverse mode laser, and Fig. (12b) involved the use of a laser output with transverse mode control. Fig. (13) is a graph of results obtained by observing the amount of attenuation behind the sample necessary for the film to be unexposed. Each error bar includes four or five such measurements. The finite steps of attenuators and fluctuations in the transmission resulted in about a x2 resolution. The vertical axis is more properly called the peak energy/$cm^2$.

The non-linear transmission results are in agreement with the idea of low loss self-induced transparency propagating pulses, but could also be explained by other mechanisms[4] such as "hole burning". With increased accuracy of theory and experiment, such measurements can perhaps be more indicative of what is happening; but in the experiments here, there are other more stringent and conclusive tests available to reveal the real nature of non-linear transmission. The self-induced transparency effect is uniquely distinguished by the observation of large pulse time delay and pulse reshaping effects. By a "time delay" it is not meant that the pulse peak merely shifts, but instead that if $I_{in}(t)$ and $I_{out}(t)$ are input and output intensities respectively, then $I_{out}(t + \frac{\eta L}{c}) > I_{in}(t)$ is observed to be the case for some time t, which would not be exhibited in the case of "hole burning". Here L is the sample length. This inequality implies that energy has been stored temporarily in the dipole system, and then returned to the field pulse. The large delay time L/V which occurs for on-resonance transparency signifies that the geometric length of the pulse in the medium is of the order of $V\tau \sim \alpha^{-1}$ for $c \gg V$, and the medium stores most of the original pulse energy.

The initial delay observations used a more primitive form of the laser than an improved version to be described later. There was no transverse mode control, and the output pulse went directly through the Kerr Cell into the sample as shown in Fig. (9). Detectors used were an S-20IT photototube and a Philco semiconductor photodiode. The output from the sample was given an extra time delay by passage through thirty feet before striking the photototube. The monitor beam excited the photototube first in time. With the use of a semiconductor detector the sequence was reversed. The semiconductor detector was placed in a plane which coincided with the image of the output surface of the sample formed by a positive lens (magnification x14).

The non-linear transmission measurements indicated a transmission loss of about 75%. The largest pulse delay should occur when the pulse width $\tau(z)$ is large, comparable to $T_2'$, and if it is held approximately constant in distance. Slight convergence of the incident light beam allows a nearly constant $\tau(z)$ by increasing the beam energy per $cm^2$ in order to compensate for beam losses. Therefore the net delay time would be given by $\alpha L\, \tau/2$, which is greater than the longest delay time $\sim T_e \log(T_e/\tau_o)$, given by Eq. (83), for a collimated beam.

This situation was arragned so that the beam diamtere converged by a factor of about 2 1/2 through the length of the sample. Delay observations under these converging beam conditions are described in Ref. 10. Figs. (14a) and (14b) illustrate examples of the first observations[10] under parallel beam conditions of pulse delay and reshaping with the simplest arrangement in Fig (9) of source, sample, and detector. A semi-conductor detector was used in the earlier converging beam investigations which detected a maximum delay of

about 60 nsec. Later delay observations were made with a new ruby laser-amplifier system which produced shorter input pulses (~ 4 nsecs). With parallel beam conditions, delays of about 10 nsec were observed.

2π Pulse Measurements

The delay measurements, referring to Figs. (14c - g) output signals, were made with a new arrangement shown in Fig. (15). The detector measured the light intensity which went through a mask in the image plane of the output end of the sample, of which a 59 micron circle was brought into focus by an f-2 lens.
With the same new arrangement, the laser-amplifier output was directed into the sample, and a filter which transmitted only one sense of circular polarization was put between the aperture stop above and a ITT S-20 photo-tube. Two ground glass surfaces in front of the phototube, combined with careful positioning of the detector, removed the possibility of serious dependence of sensitivity upon the orientation and position of the detector. Measurements of the pulse height and half-width were made of sample output pulses. Prior to these measurements the phototube was calibrated by observing the output current produced by a weak incident incoherent light beam which was spectrally filtered (6940A - 200A wide band pass filter). The input intensity was measured with a calibrated Epply thermopile. The calibration was checked by measuring output currents produced by the phototube when irradiated by a Q-switched laser pulse. The measurements were compared with ballistic calorimeter measurements with agreement within 20%. The measurements of the Epply thermopile were chosen. The final calibration was estimated to be accurate to within 10% and was represented in terms of the vertical displacement of a 519 Oscilloscope trace, measuring 71.5 watts/cm. The time resolution of the ITT photodetector was judged to be adequate for these measurements by virtue of the observed 0.5 nsec

half-width pulse response of the detector to a mode locked Nd laser pulse. Transmission through the various optical elements was calculated to be 59.5%. The effect of the sample end reflection was taken to be a transmission loss of 7.5%.

With the sample temperature near $4.2^{\circ}$ K a number of sample output pulses were recorded. Fig. (16) illustrates typical output signals which provide data for the graph in Fig. (17). The graph plots pulse height vs. pulse width for pulses selected by the following criteria: the pulse had to have precisely two points of inflection, one on the leading edge, one on the lagging edge. For example, the pulse in Fig. (16b) was accepted but a pulse shown in Fig. (16a) was not accepted. The value of $p^2/\eta$ for $Cr^{+3}$ in ruby was computed from the integral absorption cross-section data by Nelson and Sturge[26] (their Table I) to be $13.34 \times 10^{-42}$ cgs units. The effective dipole moment p in the measured quantity $p^2/\eta$ is not the isolated dipole moment of $^4A_2(\pm\frac{1}{2}) \leftrightarrow \bar{E}(2E)$ transition in $Cr^{+3}$, but is instead its shielded value. Use of this value is the equivalent of expressing the interacting field $\mathcal{C}$ as the local field at the site of the dipole in the host medium $Al_2O_3$. With this value of $p^2/\eta$ the relation between peak power $S_P$ in megawatts and the pulse width $\tau_{HW}$ (full width at half maximum intensity) of a circularly polarized output $2\pi$ h.s. pulse is $S_P = \frac{61.6}{\tau_{HW}^2} MW/cm^2$, where $\tau_{HW}$ is the number of nanoseconds which defines the full width of the observed pulse at half-maximum intensity. The pulses have a measured area always less than the ideal $2\pi$ value, roughly between $\pi$ and $2\pi$. The theoretical logarithmic plot of $S_P$ versus $\tau_{HW}$ is shown in Fig. (17). It is also significant that no unique relationship is measured between the peak pulse energy and pulse width, as shown in Fig. (17), although the product of peak pulse heights over a broad

range of values, with their corresponding pulse widths, still yield a restricted range of areas.

Within the plane wave model a number of causes can be invoked to account for deviations from the ideal $2\pi$ area value. In ruby both the right and left circularly polarized traveling waves interact with $Cr^{+3}$ ions. Consider, for example the circularly polarized input pulse of a given sense of rotation ($\sigma+$), which is above the $\pi$ area threshold condition. It will partially convert to the opposite sense of rotation ($\sigma-$) because of

birefringence (the c axis of the ruby crystal deviates from the cylindrical axis throughout its length by several degrees). The small pulse area associated with the $\sigma$ component will be below the $\pi$ area threshold for self-induced transparency and be absorbed. This constitutes a loss mechanism which drains energy away from the $\sigma+$ component which initially exhibits the transparency. In ruby additional complications result from the dynamic mixing of magnetically degenerate states of the $Cr^{+3}$ optical levels, where the mixing is caused by the local magnetic fields of neighboring $Al^{27}$ nuclear moments. Another contribution to non-ideal $2\pi$ area behaviour is the fact that plane wave conditions did not persist in view of the properties of pulse stripping and diffraction effects discussed previously. The lack of uniform pulse intensity profile, even for plane wave behaviour, is also a contributing factor, as mentioned previously in regard to Eq. (62).

The major cause of the consistent deviation of measured output pulses from the $2\pi$ area in Fig. (17) is the fact that the output pulses exist in the form of small filaments, smaller than indicated in Fig. (12). The aperture stop areas used to calibrate the response of the detecting system were not in general completely covered by the output pulse cross-sectional profile areas. The filament areas were less than the stop area, and sometimes a fraction of the filament area would fall outside of the stop area boundary. An inspection of the situation would account for measured pulse-area angles less than $2\pi$ and for the deviation of the average slope of measured points in Fig. (17) away from the line slope in the case of $\theta = 2\pi$.

Mention should be made of some of the uncontrolled experimental aspects of the ruby laser source and sample system. It was noticed that strain induced birefringence of the ruby sample at liquid helium temperatures was

considerable in its influence upon the transparency effect. When the strains were reduced by mechanically clamping the sample less tightly at the exit end, the transparency threshold condition was increased. With strains minimized as much as possible, the sample output beam appeared to be quite uncollimated and the beam came out in a cone of about 5 to $10^{o}$. At a minimum sample strain a high resolution photograph of the transverse variation of the output is shown in Fig. (18). The input contained filament diameters typically about 10 to 30 microns. It is clearly seen that the plane wave conditions in the experiment are violated to some degree. In the presence of high sample mechanical strain, it is suspected that the primary interaction region at resonance between $Cr^{+3}$ ions and the light took place near the output end of the sample where the end clamp produced a predominant mechanical strain. Mechanical compressive strain on ruby shifts the absorption line toward lower frequencies. This probably allowed the sample resonance at the rod exit end region to be more easily tuned to the laser source, because the laser source frequency always tends to be on the low side of exact resonance because of flash lamp heating. When the strain is relieved, the light interacts with essentially the entire sample length, and because the beam forms small diameter filaments, diffraction effects then become more important. The diffraction effect reduces the power along the filaments, and therefore demands a higher driving power in the input to achieve the transparency threshold condition.

The question as to why small filaments persist in these preliminary transparency effects over long distances may possibly be answered in terms of pulse stripping, focusing, and diffraction effects which are present simultaneously. The power levels in a filament in these experiments are small

compared with that required for self-trapping in sapphire. Nevertheless, although the conditions for plane wave propagation in the experiment are violated, yet the gross experimental results are predicted by the plane wave theory of self-induced transparency.

## IX. CONCLUSIONS AND DISCUSSION

The self-induced transparency effect has been experimentally confirmed, and has been analyzed mainly on the basis of ideal assumptions. An undamped ensemble of dipole oscillators is chosen as representative of an inhomogeneously broadened two level quantum mechanical system which is at or near resonance with a pulse of plane wave radiation. The effect of phenomenological relaxation damping times is accounted for to first order in the ratio of short pulse width times to long damping times. Experiments with ruby indicate that the plane wave condition is violated, and that transverse instabilities exist in the beam. Intensity variations across the profile of the pulsed laser input beam are possibly associated with these instabilities and impose further deviations from the predicted $2\pi$ h.s. area and shape of output pulses. These complications arise from a number of simultaneous effects such as beam diffraction, frequency and phase modulation, and erratic laser pulse outputs. Future investigations of of the transparency effect must cope with deviations from plane wave conditions, particularly with regard to the influence of transverse properties of the beam as discussed, for example, concerning a single transverse mode relating to Eq. (65). Of course the plane wave condition is more easily satisfied in transparency experiments with systems where the dipole moment p is large, and promises to be a reasonably obeyed condition in experiments where the power required for a $2\pi$ h.s. pulse is not too large, as in the work of Patel and Slusher[12].

In spite of a number of uncontrolled aspects mentioned above, the experimental results indicate that propagating transparency type pulses do exist as strikingly symmetric output shapes which are remarkably stable against non-linear disturbances caused by frequency modulation, phase shift, and amplitude modulation. A rigorous mathematical proof of the stability of the $2\pi$ h.s. pulse with these perturbations taken into accoount is, however, presently lacking.

There are indications that there may be breakup of input pulses of area $A > 3\pi$ into separate $2\pi$ pulses. The nature of the frequency mode distribution of the injected pulses may also give rise to separate $2\pi$ pulses, where each pulse has a different center frequency (e.g. the output illustrated by Fig. 16-d). Single output pulse areas are measured to be in a range between $\pi$ and $2\pi$, but this range may be attributed to the difficulty of averaging the pulse intensities over a sufficiently small region. The final pulse outputs are consistent with the notion that they are made up of a superposition of several $2\pi$ h.s. pulses if the plane wave condition is obeyed, whether or not the input is frequency modulated. The nature of the transverse output variations is not yet understood.

The Faraday rotation effect has been discussed[27] in its relation to transparency in ruby. This effect results from the dependence of the wave vector k, given by Eq. (57), upon the shift of the spectrum $g(\Delta\omega)$ with an externally applied magnetic field, if the optical levels are made up of Zeeman degenerate states. In ruby each participating level is doubly degenerate. If the degeneracies are slightly lifted by a magnetic field, and the center of the $g(\Delta\omega)$ line is tuned previously in zero field to the applied optical frequency $\omega$, a plane polarized input pulse should transform into a plane polarized output pulse with, however, the plane of polarization rotated through an

anomalously large angle. It is instructive and realistic to point out what the actual experimental conditions would impose upon this effect. Exact tuning at the center of spectral distribution was not the case in our ruby experiments. If the light frequency drives the resonance on one side of the peak of $g(\Delta\omega)$, the plane wave model predicts that right and left circularly polarized $2\pi$ h.s. pulses will experience different wave vectors, leading to a Faraday rotation, and will also travel at different pulse velocities. Consequently, the right and left circularly polarized $2\pi$ h.s. pulses will possibly overlap at the output so that the tail of one pulse overlaps with rise of the other pulse. The output would then first appear as a function of time to be circularly polarized in one sense, become elliptically polarized as the two pulses begin to overlap, become linearly polarized when the two pulse intensities are simultaneously equal, again become elliptically polarized, and finally become circularly polarized. The two pulses would become well separated when about a radian of rotation is achieved. If the field intensity is not uniform across its profile an added complication is introduced because of pulse self-focusing which the above argument ignores.

A number of special cases of asymptotic pulse behaviour in an inverted two level amplifying system have been examined by others[23], and the one case by us in this paper. The transparency mechanism plays a role in the pulse shaping and steepening process before asymptotic limits are reached, and should serve to predict as well certain asymptotic limits within the scope of its assumptions.

We conclude by posing the question: Are there any unknown long term transient effects concerning the interaction of coherent radiation with matter which may reveal themselves only after very careful experiment?

It is not inconceivable, for example, that some aspect of self-induced transparency might exist in interstellar space, where particle densities are very low (see Appendix A), and relaxation times are very long. Questions of this nature must follow if care is taken not to accept the predictions of rate equations under conditions where transient coherence effects may be important.

Acknowledgments

We wish to thank R. Fisher, T. Pierce, L. Riley, R. Slusher and Y. Shen for helpful discussions and T. Pierce for his assistance in making many of the measurements. One of us (S. L. McCall) gratefully acknowledges National Science Foundation Fellowship support; and the other (E. L. Hahn) thanks the A. C. Miller Institute of Basic Science for a Professorship during a portion of this work. We are very grateful for the assistance of the Inorganic Materials Research Laboratory in making available especially expensive laboratory apparatus.

This work was supported in part by the United States Atomic Energy Commission.

## APPENDIX A

For the induced electric polarization to be represented by a continuum, the relevant volume to be used for averaging must contain a large number of radiating dipoles so that the fractional statistical variation of this number is then small. A simple argument shows that a volume $\sim \lambda\alpha^{-2}$ should be chosen. Consider a small region in the plane wave where a coherent source of dipoles is spread over a circle of diameter d which radiates into a diffraction cone of apex angle $\phi \approx \lambda/d$. The electric field envelope $\mathcal{E}$ changes appreciably in a length $\alpha^{-1}$. The pertinent averaging volume is therefore determined by the distance $\alpha^{-1}$ over which diffraction occurs, and the condition that the beam spread in diameter, given by $\phi\alpha^{-1}$, is approximately equal to d itself. Thus $d \approx \sqrt{\lambda/\alpha}$, which determines an effective radiating volume $\approx \lambda\alpha^{-2}$. The effective number $N$ of radiating dipoles in this volume is not $N\lambda\alpha^{-2}$, but must be given by

$$N = N\lambda\alpha^{-2}T_2^*/\tau \gg 1, \tag{1-A}$$

which is to be large. The extra factor $T_2^*/\tau$ arises because the bandwidth $1/\tau$ of the driving pulse excites the fraction $T_2^*/\tau$ of all dipoles in the spectrum. One can define $T_{1se} = \frac{3\hbar c^3}{8p^2\omega^3}$ to be the inverse of the Einstein spontaneous emission rate. Upon applying the definition of $\alpha$ in Eq. (36) to Eq. (1-A), the inequality becomes

$$\frac{4\pi}{3}\frac{T_{1se}}{\tau}\frac{1}{\alpha\lambda} \gg 1. \tag{2-A}$$

It is already assumed that

$$\alpha\lambda \ll 1 \tag{3-A}$$

because of small backscattering, and furthermore

$$\tau \ll T_2', \tag{4-A}$$

so that certainly it is true that $\tau \ll T_{1se}$, because of the condition $T_2' \lesssim T_{1se}$. Therefore the inequality (2-A) is a consequence of these assumptions. The inequalities (3-A) and (4-A) limit the maximum value that one can choose for N, which, surprisingly, makes the inequality (1-A) less strong as N increases because $\alpha$ is proportional to N. Conversely, the inequality (1-A) becomes greater as N decreases and the relevant radiating volume becomes larger. The approximation that the light is a plane wave, however, breaks down if N becomes too small.

An alternative to the expression Eq. (2-A) is to note that we can write Eq. (1-A) as $N = (N\lambda^3 T_2^*/\tau)\,\frac{1}{(\lambda\alpha)^2} \gg 1$. From Eq. (3-A) the factor $(\lambda\alpha)^2$ represents approximately the very small fraction of the total propagating energy which is backscattered, although $N\lambda^3 T_2^*/\tau$ may represent as little as one or a fraction of a radiating dipole, on the average, within a wave length. In the experiments of Patel and Slusher,[12,25] the continuum description possibly applied to as few as one radiating $SF_6$ molecule per $\lambda^3$ volumn.

## APPENDIX B

The effect of $T_2'$ and $T_1$ upon the pulse area is now considered. In Eqs. (22), (24), and (25) replace v by v $\exp(t/T_2')$, u by u $\exp(t/T_2')$, and $\mathcal{E}$ by $\mathcal{E}\exp(t/T_2')$. Thus, Eqs. (24) and (25) are unchanged but Eq. (26) is not. With no damping the area theorem proof used Eqs. (26) only to evaluate $v(\Delta\omega=0,\ t \to \infty)$. A similar derivation before this final evaluation now yields

$$\frac{d}{dz}\left\{\kappa\int_{-\infty}^{\infty}\mathcal{E}(t';z)e^{t'/T_2'}dt'\right\} = -\left(\frac{\alpha}{2Np}\right)\lim_{t\to\infty}[v(\Delta\omega=0,\ z,t)e^{t/T_2'}], \qquad (1\text{-B})$$

where t in this appendix is the retarded time $t-\eta\, z/c$.

If the left hand side of Eq. (1-B) converges, which requires that $\mathcal{E}$ must decrease faster than $e^{-t/T_2'}$, then this result may be regarded as an exact generalization of the area theorem to account for homogeneous broadening. Eq. (1-B) can be expanded in powers of $1/T_2'$, where only the first order correction will be considered. Let a delay time $t_c(z)$ be defined such that

$$\int_{-\infty}^{\infty}\mathcal{E}(t';z)[t'-t_c(z)]dt' = 0, \qquad (2\text{-B})$$

where $t_c(z)$ is proportional to the first moment of t relative to $t = 0$.

Then to first order in $T_2'^{-1}$

$$\frac{d}{dz}\left\{\int_{-\infty}^{\infty}\kappa\mathcal{E}(t';z)e^{t'/T_2'}dt'\right\} = (1 + t_c/T_2')\frac{dA}{dz} + \frac{A}{T_2'}\frac{dt_c}{dz}. \qquad (3\text{-B})$$

Furthermore, it may be verified that the following is the solution, at exact resonance $\Delta\omega=0$, to the optical Bloch Eqs. (25) and (26) to first order in $1/T_2'$, $1/T_1$:

$$\frac{v}{Np} = \left\{1 + \int_{-\infty}^{t}\left[\kappa\mathcal{E}(t')\left(\frac{1}{T_2'} - \frac{1}{T_1}\right)t'\sin 2\varphi(t') + \frac{1}{T_1}\mathcal{E}(t')t'\sin\varphi(t')\right]dt'\right\} e^{-t/T_2'}\sin\varphi(t)$$
$$+ \cos\varphi(t)\left\{\int_{-\infty}^{t}\left[\kappa\mathcal{E}(t')\left(\frac{1}{T_2'} - \frac{1}{T_1}\right)t'\cos 2\varphi(t') + \frac{1}{T_1}\mathcal{E}(t')t'\cos\varphi(t')\right]dt'\right\}e^{t/T_2'}; \qquad (4\text{-B})$$

$$\frac{W}{(N\hbar\omega_o/2)} = -1 + e^{-t/T_1} - \cos\varphi(t)\left\{1 + \int_{-\infty}^{t}\left[\kappa\mathcal{E}(t')\left(\frac{1}{T_2'} - \frac{1}{T_1}\right)t'\sin 2\varphi(t') + \frac{1}{T_1}\kappa\mathcal{E}(t')t'\sin\varphi(t')\right]dt'\right\}e^{-t/T_1}$$
$$+ \sin\varphi(t)\left\{\int_{-\infty}^{t}\left[\kappa\mathcal{E}(t')\left(\frac{1}{T_2'} - \frac{1}{T_1'}\right)t'\cos 2\varphi(t') + \kappa\mathcal{E}(t')\frac{1}{T_1}t'\cos\varphi(t')\right]dt'\right\}e^{-t/T_1}.$$

Combining Eqs. (4-B), (3-B), and (1-B) leads to the result

$$\left(1 + \frac{t_c}{T_2'}\right)\frac{dA}{dz} + \frac{A}{T_2'}\frac{dt_c}{dz} = -\frac{\alpha}{2}\sin A\left\{1 + \int_{-\infty}^{\infty}\left(\frac{1}{T_2'} - \frac{1}{T_1}\right)t\kappa\mathcal{E}\sin 2\varphi dt + \int_{-\infty}^{\infty}\left(\frac{\kappa\mathcal{E}t}{T_1}\sin\varphi\right)dt\right\} - \frac{\alpha}{2}\cos A\left\{\int_{-\infty}^{\infty}\left[\kappa\mathcal{E}\left(\frac{1}{T_2'} - \frac{1}{T_1}\right)t\cos 2\varphi + \frac{\kappa\mathcal{E}t}{T_1}\cos\varphi\right]dt\right\} \qquad (5\text{-B})$$

Eq. (5-B) is a generalization of the area theorem to first order in $\tau/T_2'$ and $\tau/T_1$. We now restrict our discussion to a pulse which has evolved to nearly a $2\pi$ h.s. pulse form. A deviation from this form will occur only because $T_1$ and $T_2'$ are not infinite. The pulse area A will differ

from $2\pi$ by a negative increment to first order in $1/T_2'$. The pulse itself differs from the ideal hyperbolic secant shape to order $1/T_2'$. In the various integrals on the right hand side of Eq. (5-B) $\xi$ and $\varphi$ may be taken to zero order. The above Eq. (5-B) then reduces to

$$\left(1 + \frac{t_c}{T_2'}\right)\frac{dA}{dz} + \frac{A}{T_2'}\frac{dt_c}{dz} = -\frac{\alpha}{2}\sin A + \frac{4\alpha\tau}{3T_2'}\sin A + \frac{2\alpha\tau}{3T_1} - \sin A. \qquad (6\text{-B})$$

For the nearly $2\pi$ h.s. pulse, let $A = 2\pi+\Delta A$, where $\Delta A$ is an area increment. To zero order, $dt_c/dz = \alpha\tau/2$, for $\tau \gg T_2^*$, as seen from Eq. (56) (transforming to the retarded time drops the $\eta/c$ term). Since $\Delta A$ is of order $1/T_2'$, keeping only terms of first order in $1/T_2'$ in Eq. (6-B) leads to

$$\frac{d(\Delta A)}{dz} = -\frac{\pi\alpha\tau}{T_2'} - \frac{\alpha}{2}\Delta A; \qquad (7\text{-B})$$

so that after a few absorption lengths

$$\Delta A(z) = -\frac{\pi\alpha}{T_2'}\int_0^z dz' e^{\frac{-\alpha}{2}(z-z')}\tau(z'), \qquad (8\text{-B})$$

which states that $\Delta A$ relaxes toward the value $-2\pi\tau/T_2'$. The fractional change of $\Delta A$ to first order in $\tau$ in an absorption length $\alpha^{-1}$ is of order $T_2'^{-1}$. Therefore, to first order,

$$A \approx 2\pi(1 - \tau/T_2'), \qquad (9\text{-B})$$

which is independent of $T_1$, in contrast with the pulse energy loss result of Eq. (79) which depends upon both $T_1$ and $T_2'$.

## REFERENCES


1. A. L. Schawlow and C. H. Townes, Phys. Rev. 112, 1940 (1958); T. H. Maiman, Nature 187, 493(1960); F. J. McClung and R. W. Hellwarth, J. Appl. Phys. 33, 828 (1963).

2. E. H. Jacobsen, Phys. Rev. Letters 2, 249 (1959); H. Bommel and K. Dransfeld, Phys. Rev. Letters 3, 83 (1959); N. S. Shiren, Phys. Rev. 128, 2103 (1962); E. H. Jacobsen and K. W. H. Stevens, Phys. Rev. 129, 2036 (1962).

3. F. J. Lynch, R. E. Holland and M. Hamermesh, Phys. Rev. 120, 513 (1962); Ref. 2, N. S. Shiren.

4. See References 88 - 110 in Bibliography by James D. Macomber, IEEE, Journal of Quantum Electronics, QE-4, 1 (1968).

5. C. L. Tang and B. D. Silvermann, Physics of Quantum Electronics, edited by P. L. Kelley; B. Lax and P. E. Tannenwald (McGraw-Hill Book Co., New York, 1966), P. 280; G. B. Hocker and C. L. Tang, Phys. Rev. Letters 21, 591 (1968); J. A. Armstrong, N. Bloembergen, J. Ducuing, P. S. Pershan, Phys. Rev. 127, 1918 (1962); N. Bloembergen and Y. R. Shen, Phys. Rev. 133, A37 (1964).

6. H. C. Torrey, Phys. Rev. 76, 1059 (1949); E. L. Hahn, Phys Rev. 77, 746 (1950); N. Bloembergen and R. V. Pound, Phys. Rev. 95, 8 (1954); S. Bloom, J. Appl. Phys. 28, 800 (1957); R. H. Dicke, Phys. Rev. 93 99 (1954); E. T. Jaynes and F. W. Cummings, Proc. IEEE 51, 89 (1963).

7. I. D. Abella, N. A. Kurnit, and S. R. Hartmann, Phys. Rev. 141, 391 (1966).

8. E. L. Hahn, Phys. Rev. 80, 580 (1950).

9. A. Beer, Ann. d. Phys. u. Chemie, 86, 78 (1852).

10. S. L. McCall and E. L. Hahn, Phys. Rev. Letters 18, 908 (1967).

11. S. L. McCall and E. L. Hahn, Bull. Am. Phys.Soc. 10, 1189 (1965).

12. C. K. N. Patel and R. E. Slusher, Phys. Rev. Letters 19, 1019 (1967).

13. A. J. DeMaria, D. A. Stetser, and H. Heynau, Appl. Phys. Letters 8, 174 (1966).

14. p is the magnitude of the x or y component of the electric dipole. In the case of excitation by circularly polarized light, it is related to the magnitude $P_T$ of the total moment with $P_T = p\sqrt{2}$ where $P_T$ is often used as the expression for the dipole moment in the optical literature.

15. R. P. Feynman, F. L. Vernon, Jr., and R. W. Hellwarth, J. Appl. Phys. 28, 49 (1957).

16. F. Bloch, Phys. Rev. 70, 460 (1946).

17. G. L. Lamb, Jr., Phys. Rev. Letters 25A, 181 (1967).

18. J. D. Jackson, "Classical Electrodynamics". Ch. 8, P. 235-267. (John Wiley and Sons, Inc., New York, London (1962).

19. A. G. Fox and P. W. Smith, Phys. Rev. Letters 18, 826 (1967); M. Bass, G. deMars and H. Statz, Applied Physics Letters, Vol 12, No. 1, 1968.

20. S. L. McCall and E. L. Hahn, Proceedings of the Physics of Quantum Electronics Summer School, June, 1968, Flagstaff, Arizona; S. L. McCall, Thesis (unpublished), University of California, Berkeley; C. K. Rhodes, A. Szoke, and A. Javan, Phys. Rev. Letters 16, 1151 (1968).

21. An integration identical to Eq. (70) evaluates the free nuclear quadrupole precession from a powered sample in zero magnetic field (M. Bloom, E. L. Hahn, and B. Herzog, Phys. Rev. 93, 639 (1954))

22. F. V. Condon and G. H. Shortley, The Theory of Atomic Sprectra, (Cambridge Univ. Press, London, 1957) Page 387.

23. J. P. Whittke and P. J. Warter, J. Appl. Phys. 35, 1668 (1964); F. T. Arecchi and R. Bonifacio, IEEE J. of Quantum Electronics QE-1, 169 (1965); J. A. Armstrong and E. Courtens, IEEE, J. of Quantum Electronics, QE-4, 411 (1968); R. Bellman, G. Bernbaum, and W. G. Wagner, J. Appl. Phys. 34, 2346 (1963).

24. F. A. Hopf and M. O. Scully, Phys. Rev. (in press).

25. C. K. N. Patel and R. E. Slusher, Phys. Rev. Letters 20, 1087 (1968).

26. D. F. Nelson and M. D. Sturge, Phys. Rev. 137, A117 (1965).
Their measured total absorption cross-section is
$\int_{-\infty}^{\infty} \sigma(\bar{\nu})d\bar{\nu} = 2.4\times10^{-19}$ cm $= \alpha/(N\pi cg(0))$ for the $4A_2(\pm\frac{1}{2}) \leftrightarrow \bar{E}(2E)$ transition, where $\bar{\nu}$ is the wave number. For observation of the response to one component of circularly polarized light, the effective number of $Cr^{+3}$ ions is N/2. The light propagates parallel to the c axis of ruby. For $\eta = 1.75$, $p = 4.8 \times 10^{-21}$ egs. units.

27. E. Courtens, Phys. Rev. Letters 21, 3 (1968).

## FIGURE CAPTIONS

Fig. 1. Pulse area plots of self-induced transparency area theorem.

(a) Branch solutions to Eq. (36) are plotted. The entry face of the medium may be at any value of z. For an absorbing (amplifying) medium with $\alpha > 0$ ($\alpha < 0$), the pulse area evolves in the direction of increasing (decreasing) distance z toward the nearest even (odd) multiple of $\pi$. Even and odd multiples of $\pi$ area solutions are respectively stable and unstable. The distance z is marked off in units of $\pi\ \alpha^{-1}$ cm for Figs. (1-a) and (1-b).

(b) Computer plots of evolution of input $\theta_o = 0.9\pi$ and $\theta_o = 1.1\pi$ pulses with distance and time. The time scale may be fixed through an arbitrary choice of electric units and the assignment of $\theta_o$.

Fig. 2. Computer plot of function F (Eq. (40)) versus area $\theta$. A flat spectrum $g(\Delta\omega)$ = constant is assumed with the condition $\tau \gg T_2^*$. The trend of oscillations toward F = 0 appears as shapes chosen approach that of a smooth symmetric pulse. Incoherent damping because of finite $T_2'$ will tend to average out the oscillations and increase the overall value of F for $\theta \geq \pi$. A flat spectrum $g(\Delta\omega)$ = constant is assumed.

Fig. 3. Sketch of rigid pendulum solutions of Eq. (47) closely related to the $2\pi$ h.s. case.

(a) The tipping angle $\varphi$ oscillates about the equilibrium position $\varphi = \pi$ for the rigid pendulum, which is given an initial potential plus kinetic energy slightly less than the critical energy (the potential energy in the upright position). The electric field $\mathcal{E} \sim \dot{\varphi}$ is shown with its corresponding oscillations.

(b) For the initial energy precisely equal to the critical potential energy, the period of oscillations is infinite, and the pendulum yields one oscillation with $\dot{\varphi}$ proportional to a single $2\pi$ h.s. field pulse.

(c) The tipping angle $\varphi$ increases indefinitely for the initial total energy slightly exceeding the critical potential energy of the upright position.

Fig. 4. Computed absorbed energy by a thin sample from a Gaussian pulse of fixed pulse width as a function of pulse area $\theta$. A flat spectrum $g(\Delta\omega)$ = constant is assumed.

Fig. 5. Trajectories of the pseudo-vector $\underset{\sim}{P}(\Delta\omega\tau)$, driven by a $2\pi$ h.s. field pulse, for various values of $\Delta\omega\tau$. The radius of the sphere is $|\underset{\sim}{P}(\Delta\omega\tau)|$ = Np. Units of W are $\kappa/\omega$.

Fig. 6. Computer plots of absorbed energy and $\mathcal{E}$ field pulse shape, versus distance and time, for a $\theta_o = 2.9\pi$ input pulse as it evolves toward a $2\pi$ pulse. The area theorem Eq. (36) requires a pulse width narrowing and peak power amplification by almost a factor of two. The absorbed energy represents energy stored in the two level system. The units are the same as in Fig. 1.

Fig. 7. Computer plots of pulse shapes versus z and t for initial input pulse areas $\theta_o$ near $4\pi$. Final individual pulse areas, which split away from the initial pulse, evolve toward $\theta(z) = 2\pi$ for $z \gg \alpha^{-1}$. The energy absorbed in the case of $\theta_o = 4\pi$ is plotted in Fig. (7-a). Pulse separations at a given z, and final $2\pi$ h.s. pulse widths $\tau$, depend upon the input pulse areas $\theta_o$ and shapes chosen. Units of $\mathcal{E}$, z, and t are as in Fig. 1.

Fig. 8. Plot of $\pi$ pulse solution of Eq. (99) for the case of an amplifying medium, valid for $z \gtrsim 4.16\alpha^{-1}$. For $z < 4.16\alpha^{-1}$ the pulses are sketched in qualitatively to show trailing oscillations which finally disappear before the "half hyperbolic secant" solutions are reached. Between labeled distance points the peak pulse amplitudes approximately doubles.

Fig. 9. Experimental arrangement for monitoring self-induced transparency pulse delay and transmission intensity.

Fig. 10.

(a) Energy level diagram of ruby laser pulse source and the target ruby sample. The $4A_2(\pm\frac{1}{2})$ level is represented as broadened to account for the inhomogeneous $g(\Delta\omega)$ spectrum. Phonon relaxation between the $2\bar{A}(2E)$ and $\bar{E}(2A)$ level is suppressed at $4.2^{\circ}$ K to avoid $T_2' \ll \tau_p$, where $\tau_p$ is the input pulse width. The ruby laser $\bar{E}(2N \leftrightarrow 4A_2(\pm\frac{1}{2}))$ output is suppressed.

(b) Sketch of ruby two level system inhomogeneous spectrum $g(\Delta\omega)$. The relative magnitudes of homogeneous $(1/T_2')$ and inhomogenous broadening $(\frac{1}{T_2^*})$ are schematically shown.

Fig. 11. Ruby laser amplifier system. The oscillator cavity was formed by the curved mirror CM and the flat feedback mirror FBM. The oscillator beam path, indicated by the single dashed line, went through the laser rod LR, the Brewster angle calcite polarizing prism CPP, the Brewster angle Kerr cell KC and the polarizing Rochon Prism RP. Two stops S force single transverse mode operation. Due to the high gains available ($\sim 10^5$ with double pass), an 85% reflective mirror RM was used inside the cavity to couple out energy. The Kerr cell was operated at a voltage so that the net feedback was about 1%, thus suppressing the unwanted $4A_2(\pm\frac{1}{2}) \leftarrow \bar{E}(2A)$ transition. The output was focused with a lens L through a very dense saturable dye solution SD, and the beam was expanded in diameter by lenses L to fill the laser amplifier rod LA. The amplifier output was recollimated to form the final output. Mirrors FM served to fold the beam back onto the bench used to support the system. Flashlamps are designated by FL.

Fig. 12a - b. Transmitted output intensity photographs of pulses indicating non-linear transmission, with indicated input and output attenuation factors. Outputs in (12-a) and (12-b) are without and with transverse mode selection respectively.

Fig. 13. Energy output versus input ruby-light transmission through sample (arbitrary units). The magnified (x14) output is attenuated until Polaroid Type-47, 3000 speed film is unexposed, thus determining peak transmitted energy/$cm^2$. Error bars represent output fluctuations presumably caused by several uncontrolled characteristics of the ruby-laser source and the finite steps in the output calibrated attenuation. The dotted datum is the transmission with the sample at room temperature, and the dashed line represents a linear transmission law.

Fig. 14. Pulse delay observations with a collimated input.

(a) Input and output laser pulses with sample at room temperature. An optical delay served to separate the two pulses. The second pulse has traveled through the sample. Sweep speed is 20 ns per division with signal from a FW 114 Model ITT vacuum photodiode.

(b) same as (a) except that the sample is thermally tuned by cooling to liquid helium and a x20 attenuator in output beam path is removed. Pictures (a) and (b) use the system shown in Fig. 9.

(c) In pictures (c) - (f) the laser amplifier system of Fig. 11 was used. Different detectors were used for observing sample input and output, with cables and a "tee" used to separate the respective signals. Sample detuned at room temperature with output magnified x5.05 and stop diameter 12 mm (2.4 mm at the sample output face) attenuated x11,2000. Time scale: 5 nsec/div.

(d), (e), (f), (g). Sample tuned at temperature ~ 4.2° K with stop diameter 0.85 mm (0.17 mm at the sample output face) and no attenuation.

The first pulse is the monitor output. The second pulse is the detector output. Cable and distance delays amounted to 13 nsec. Cable reflections occur at the far right. Time scale: 5 nsec/div.

Fig. 15. Apparatus used for pulse area measurements. The sample output passed through lens 1 which formed an image of the sample output end E in the plane of the stop. The output through the stop aperture was collimated and passed through a circular wave polarizing system with the mask M blocking the unwanted component. The f-number of the system was limited by the output dewar windows to a value of about f = 2.

Fig. 16. Typical oscillographs of transmitted light pulses. Oscillograph (a) was not acceptable for pulse area measurements, while oscillographs (b) and (c) were acceptable. Oscillograph (c) was considered to be two separate pulses. When two separate pulses were observed, the trailing pulse always had a smaller measured pulse area. Occasionally an oscillograph similar to (d) was recorded. (d) agreed well with the idea that the output was two $2\pi$ h.s. pulses of different frequencies. Time scale: 5 nsec/div.

Fig. 17. Logarithmic plot of peak power versus pulse width. The circles represent points obtained from measured pulse widths and areas. The experimental error, apart from averaging over the 59 micron circle, is small in comparison with the data scatter.

Fig. 18. Photographs of the sample output intensity. The photograph in the upper left corner is the result of a resolution test. The other three photographs are output intensity photographs. The scale represents 59 microns at the photographic magnification of x90.

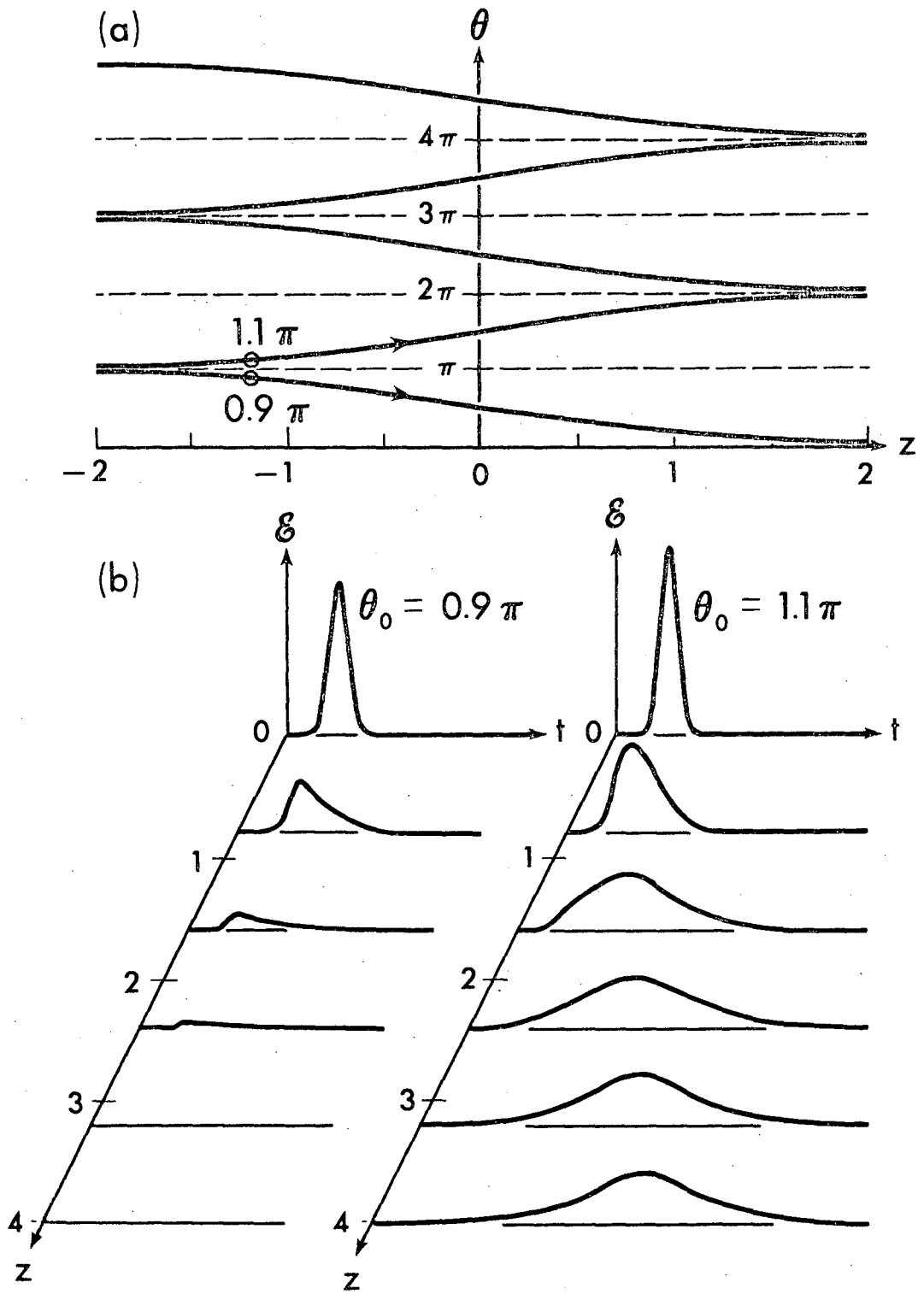


XBL695-546

Fig. 1

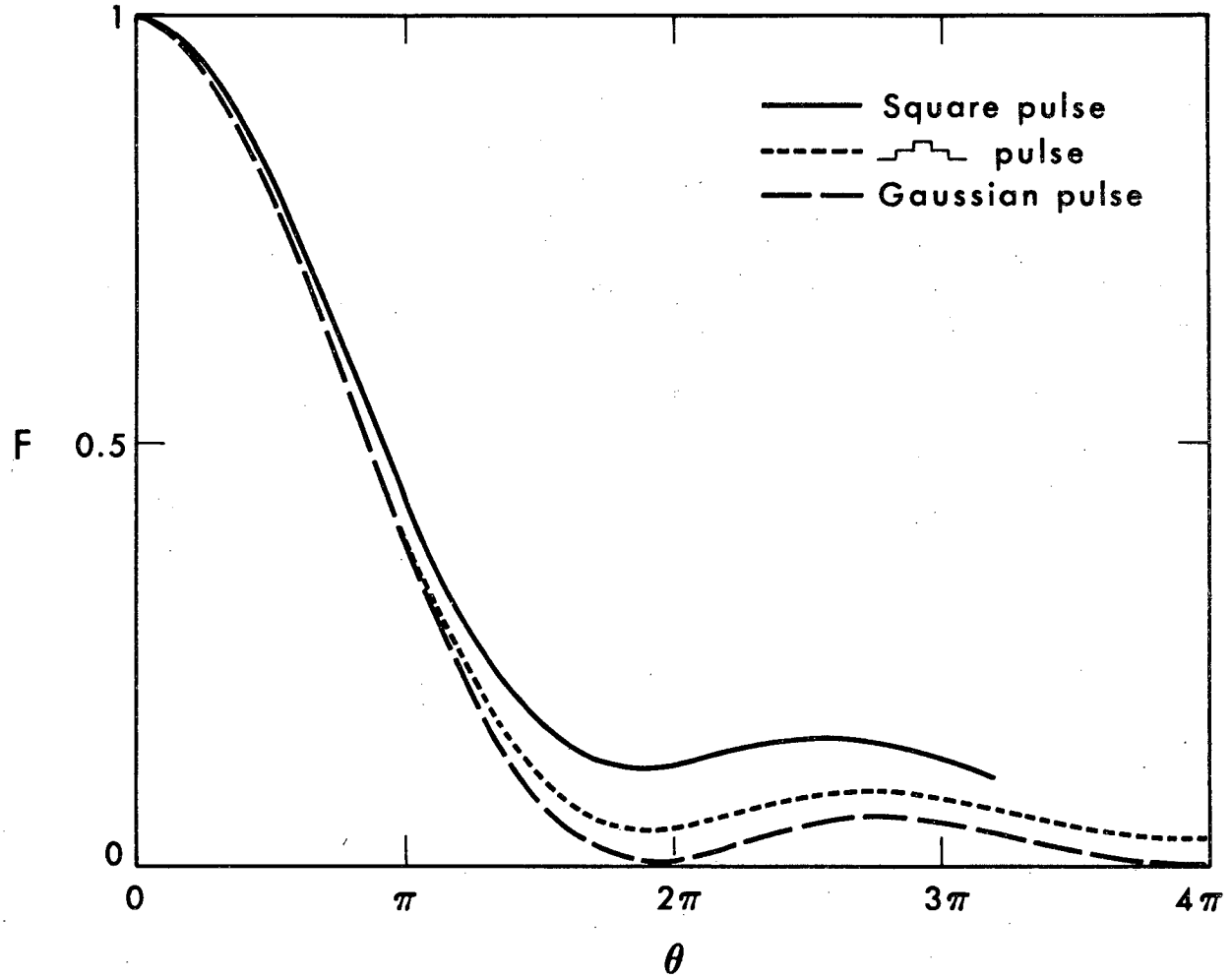


XBL695-547

Fig. 2

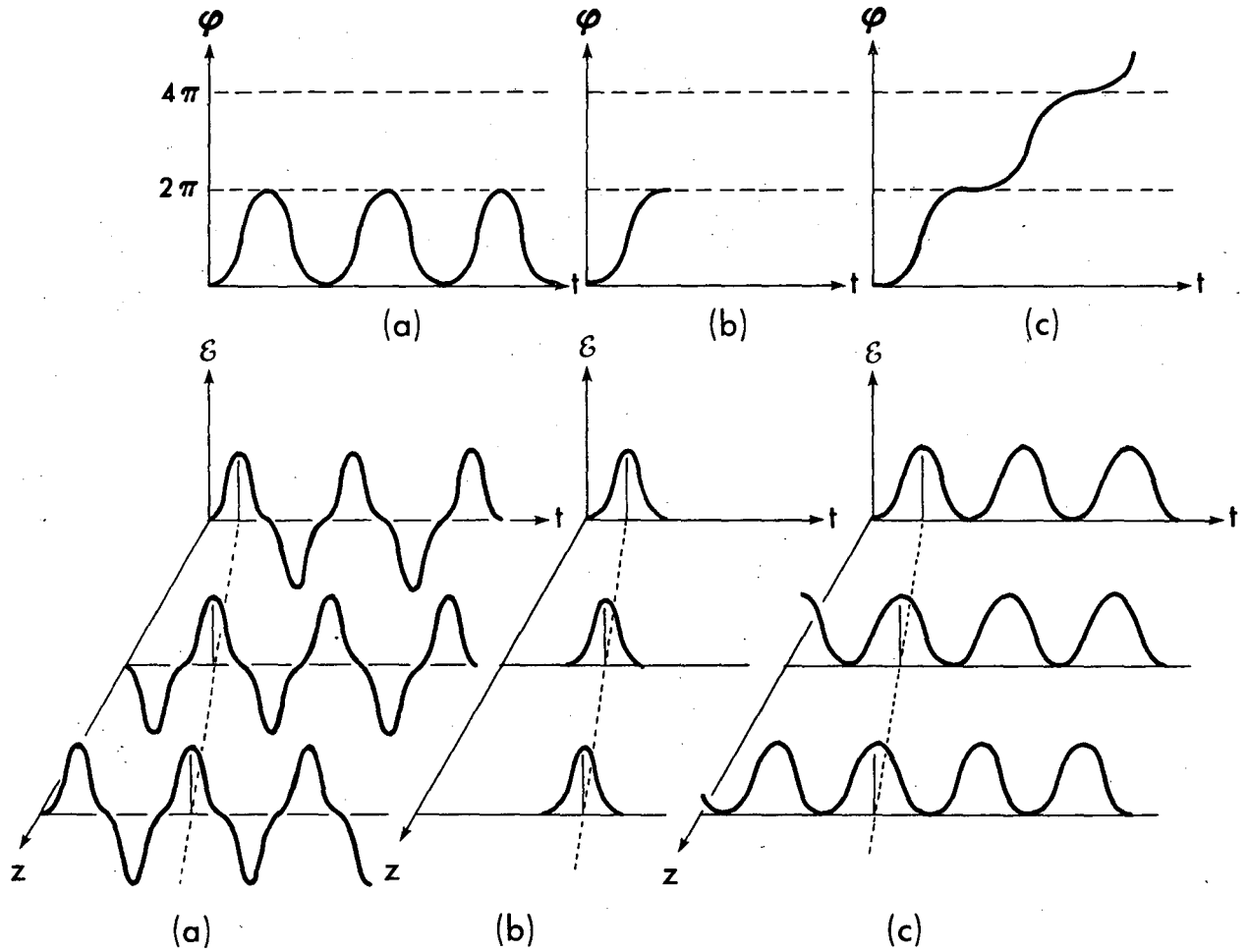


XBL695-548

Fig. 3

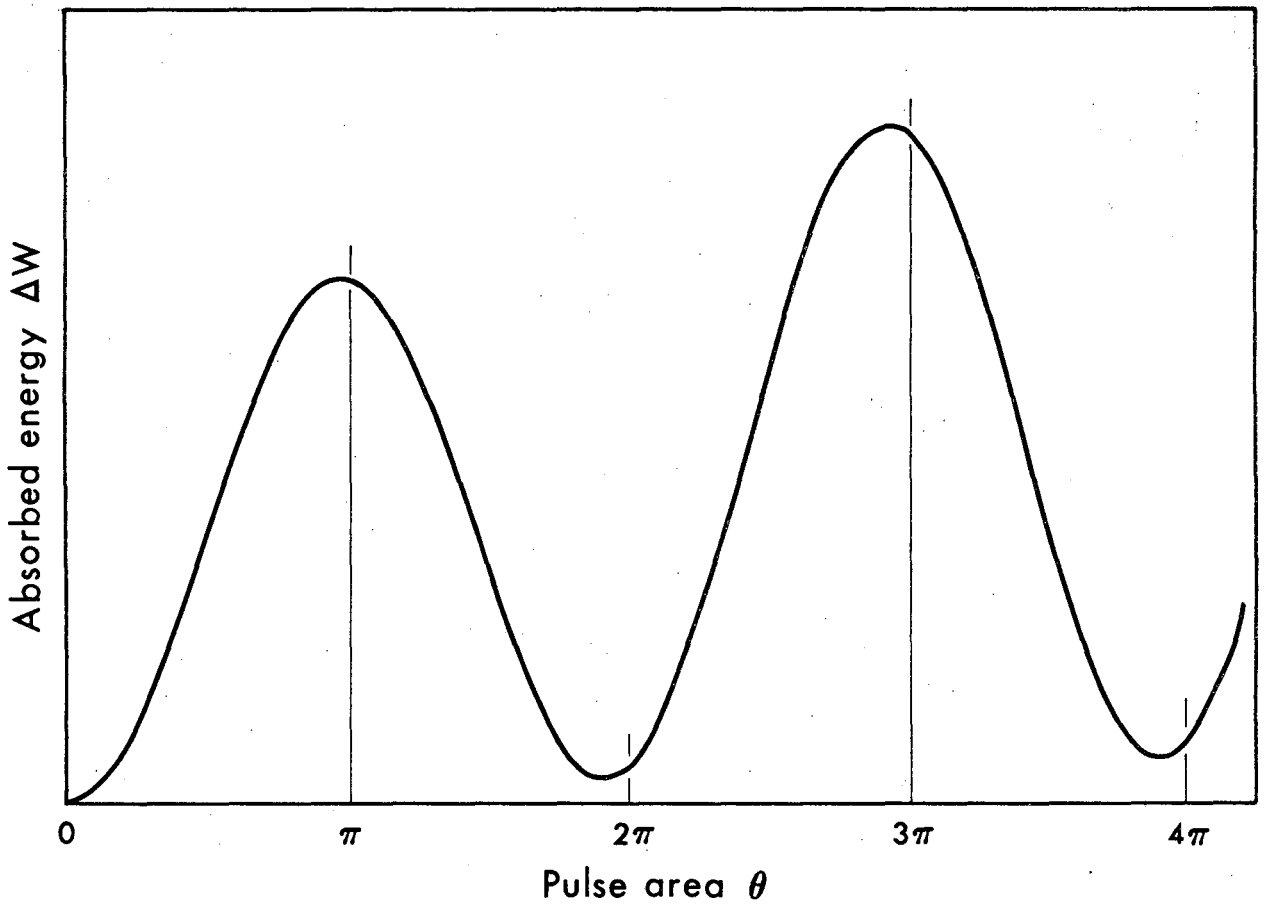


XBL695-549

Fig. 4

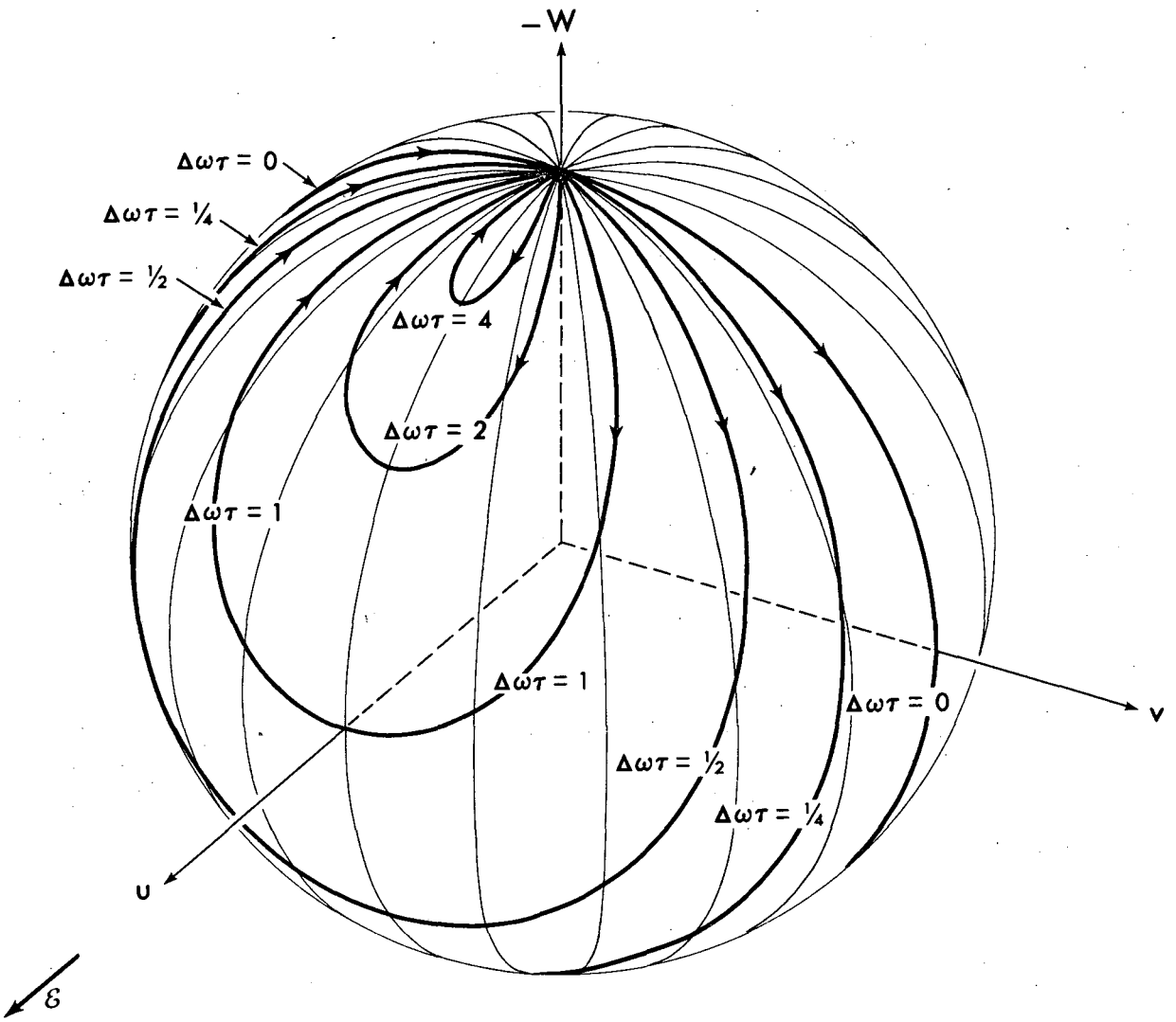


XBL695-550

Fig. 5

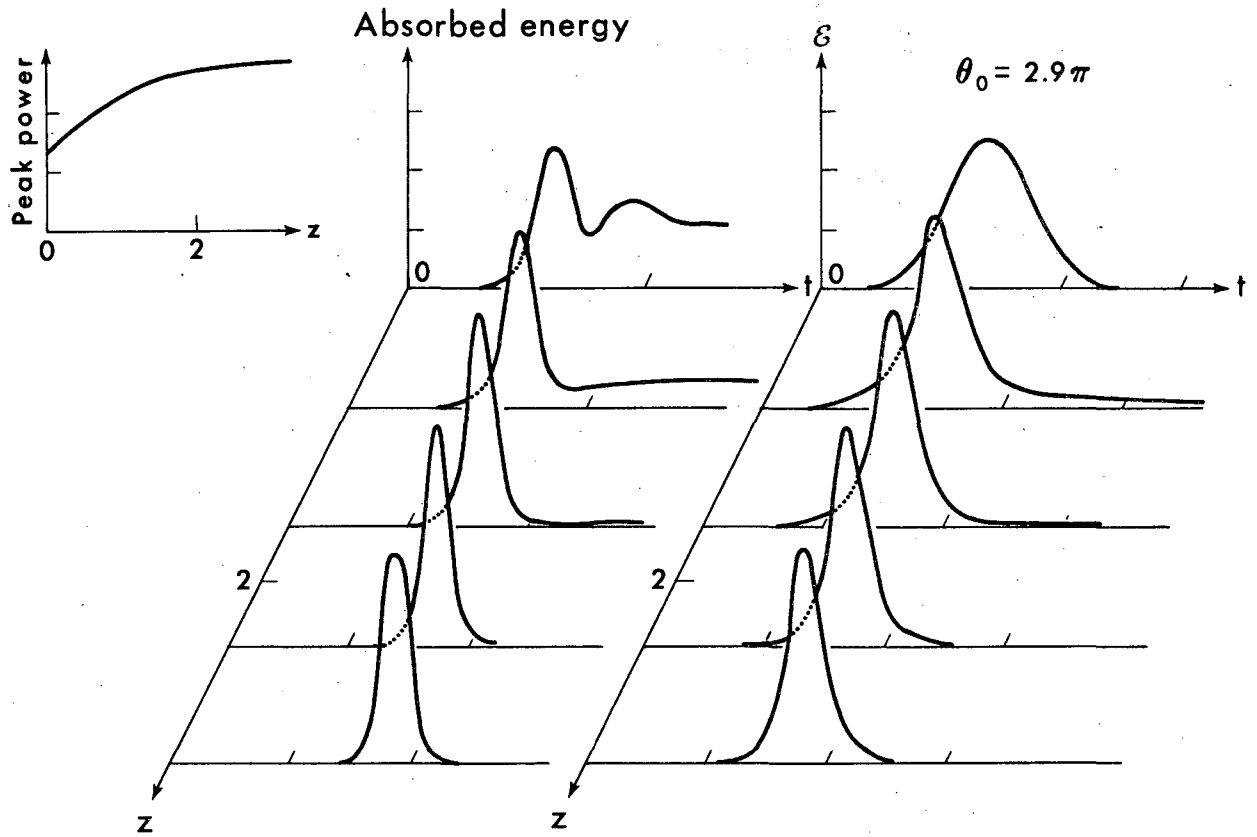


XBL695-551

Fig. 6

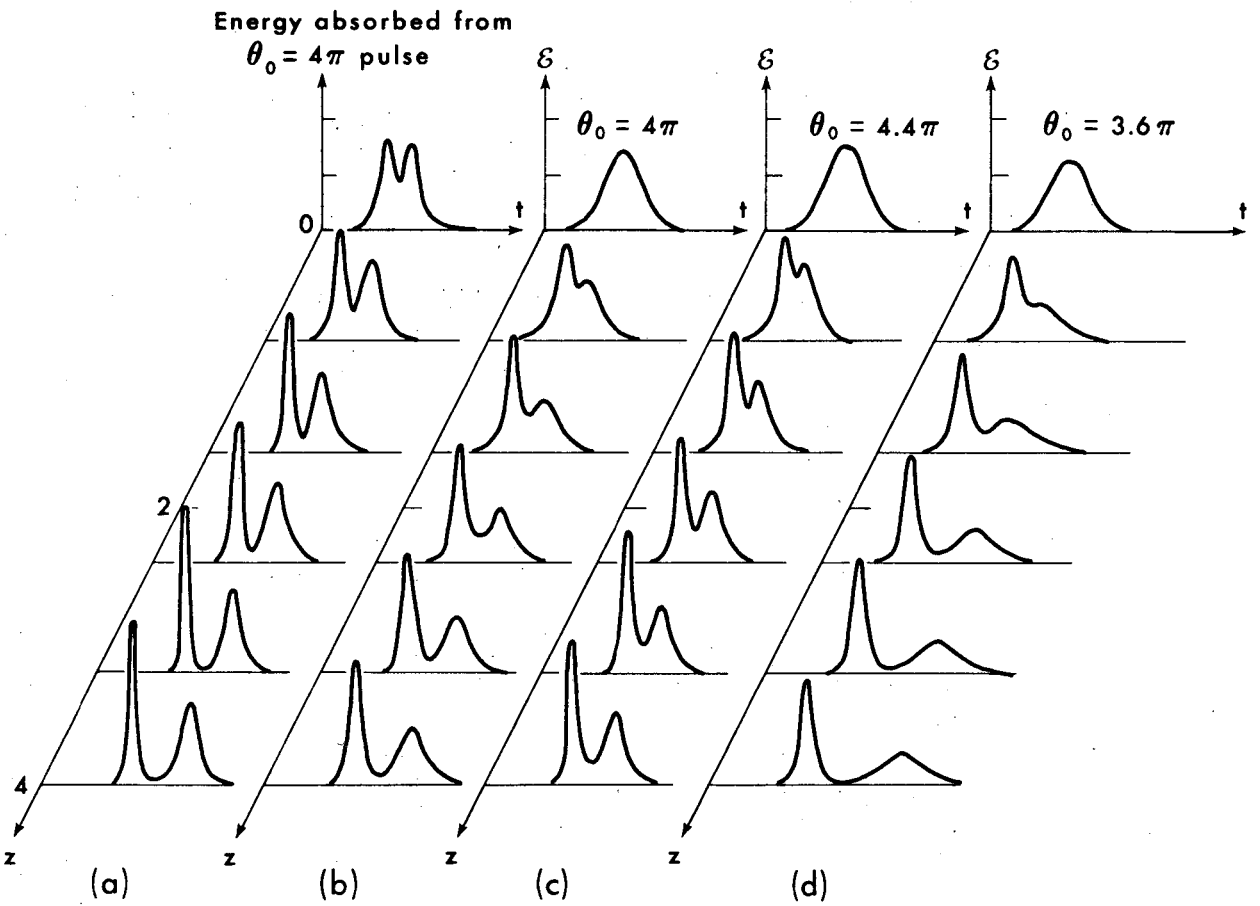


XBL695-552

Fig. 7

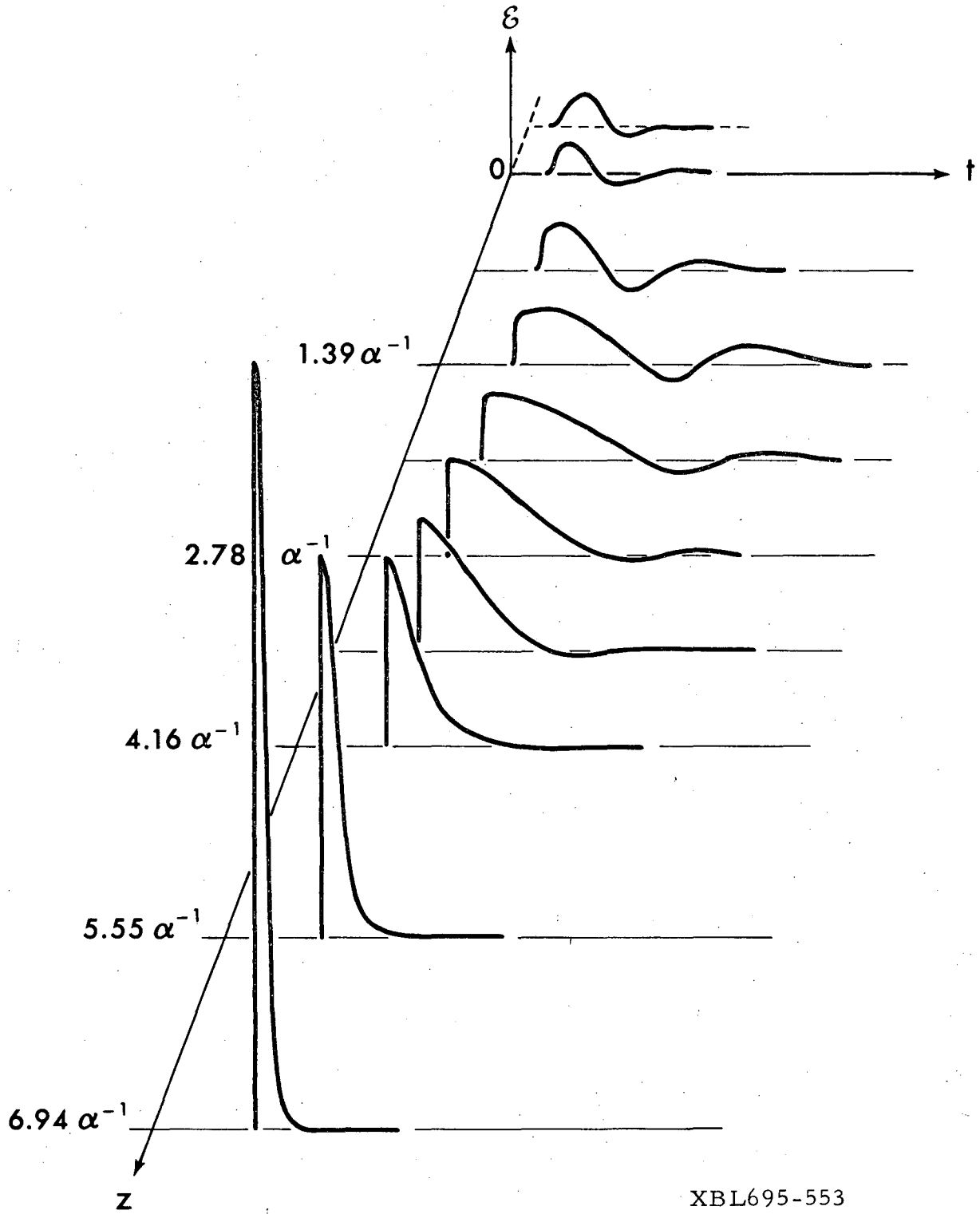
$\mathcal{E}$
0
t
$1.39\,\alpha^{-1}$
$2.78\ \alpha^{-1}$
$4.16\,\alpha^{-1}$
$5.55\,\alpha^{-1}$
$6.94\,\alpha^{-1}$
z
XBL695-553

Fig. 8

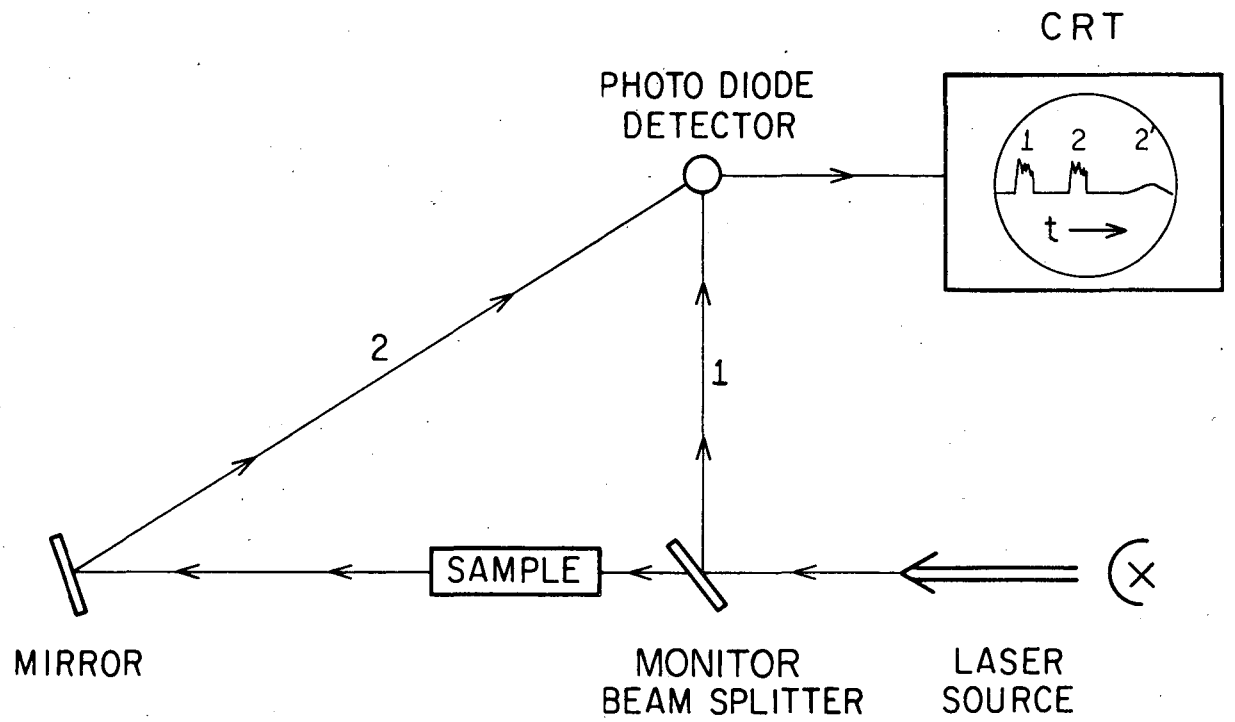


XBL695-554

Fig. 9

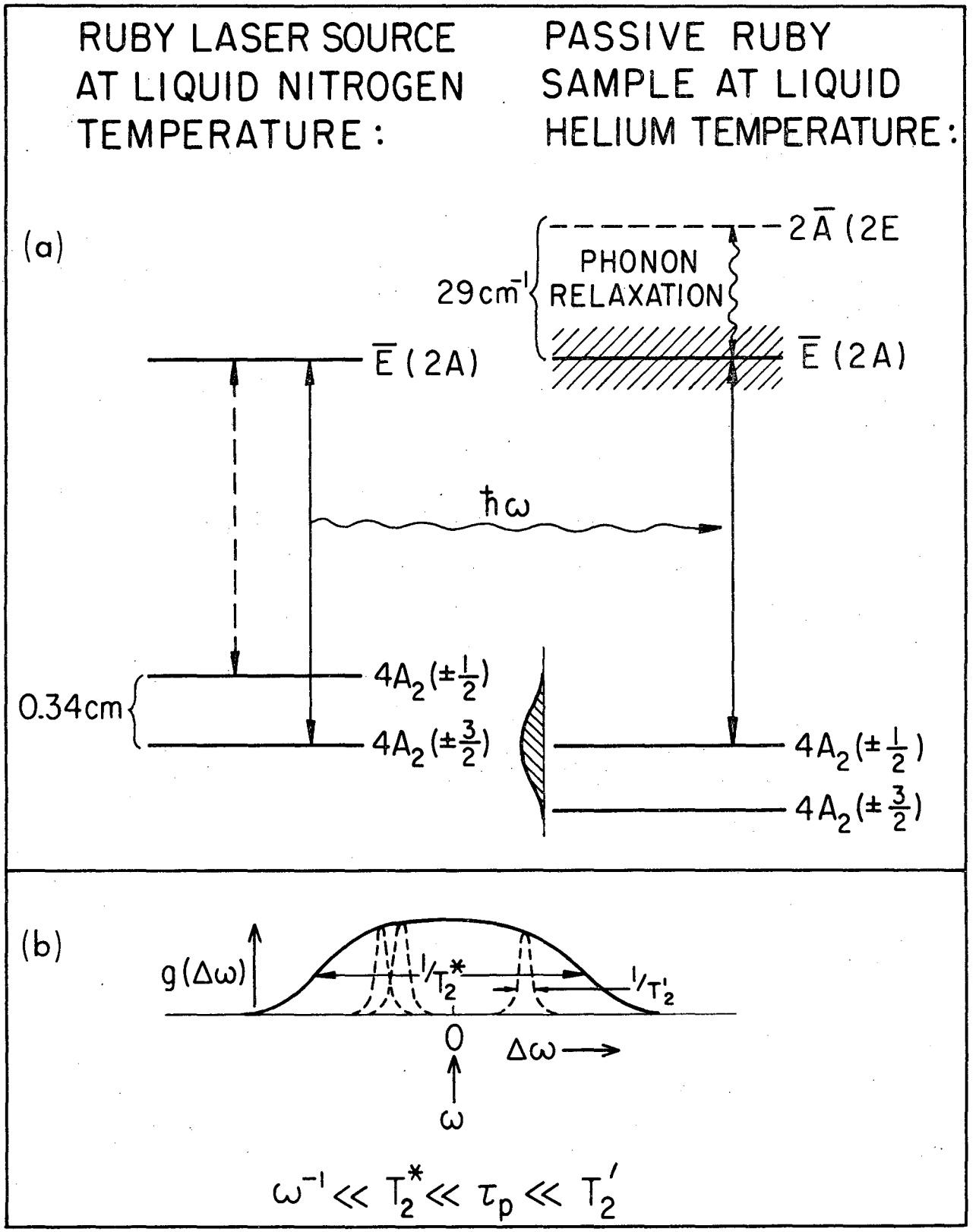


XBL695-555

Fig. 10

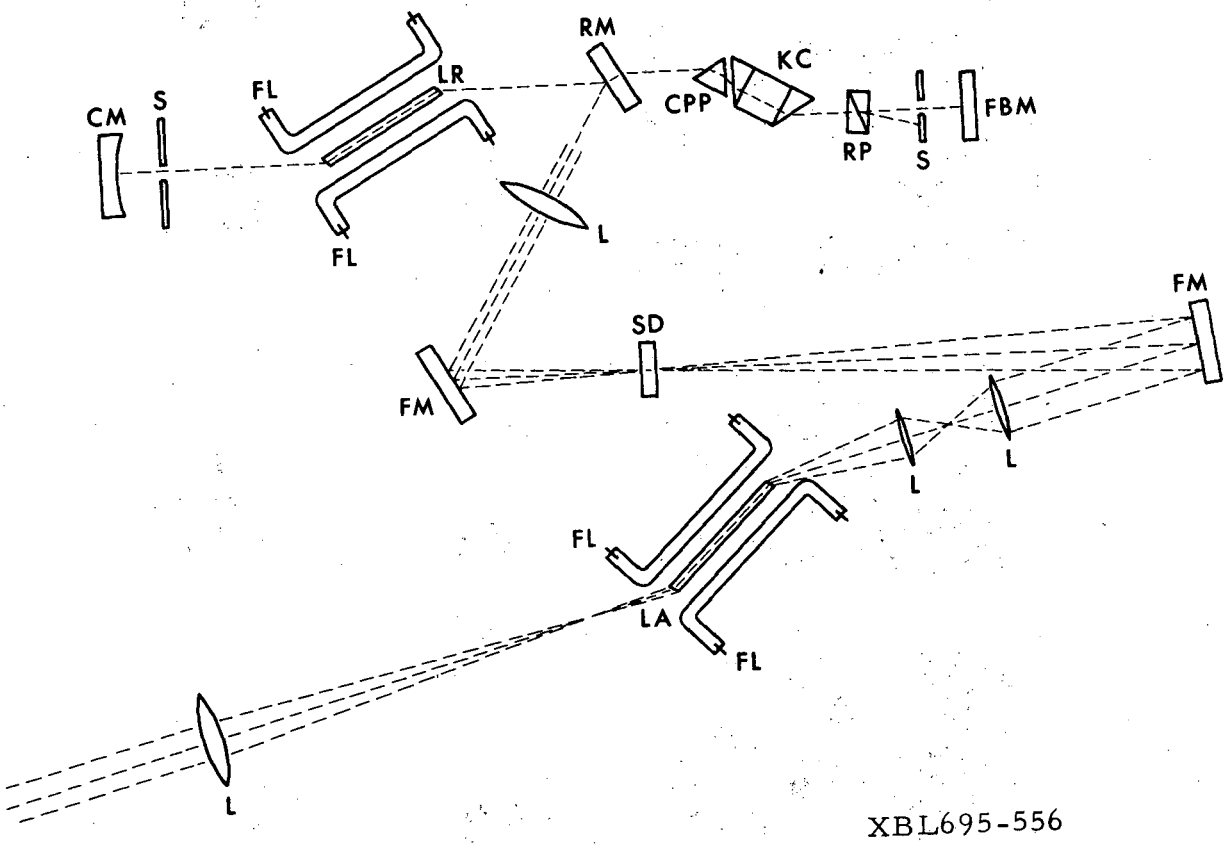


Fig. 11

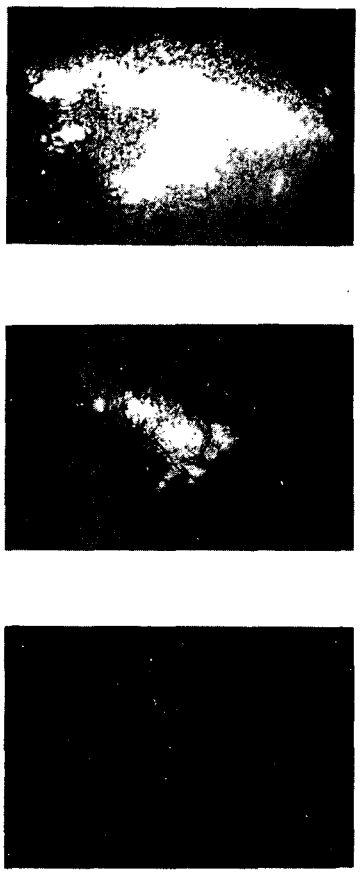

| IN | OUT |
|---|---|
| $T_0$ | $\frac{1}{\times 6.3}$ |
| $\frac{T_0}{\times 2.1}$ | $\frac{1}{\times 2.1}$ |
| $\frac{T_0}{\times 6.3}$ | $\frac{1}{\times 1}$ |

XBB 695-3383

Fig. 12a

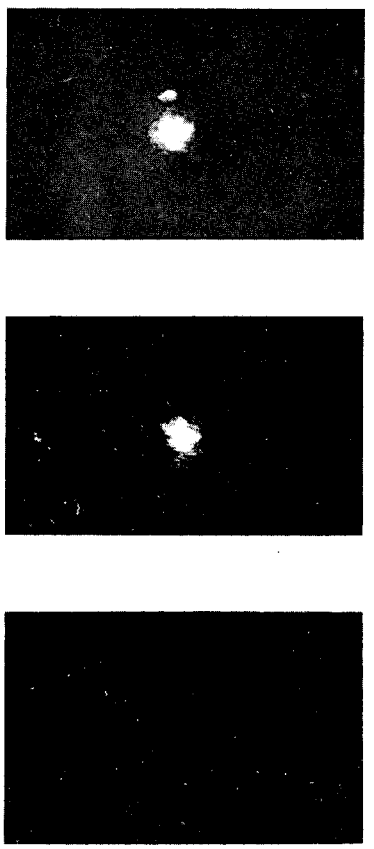

| IN | OUT |
|---|---|
| $T_0$ | $\frac{1}{2.1\times6.3}$ |
| $\frac{T_0}{\times2.1}$ | $\frac{1}{\times6.3}$ |
| $\frac{T_0}{\times6.3}$ | $\frac{1}{\times2.1}$ |

XBB 695-3384

Fig. 12b

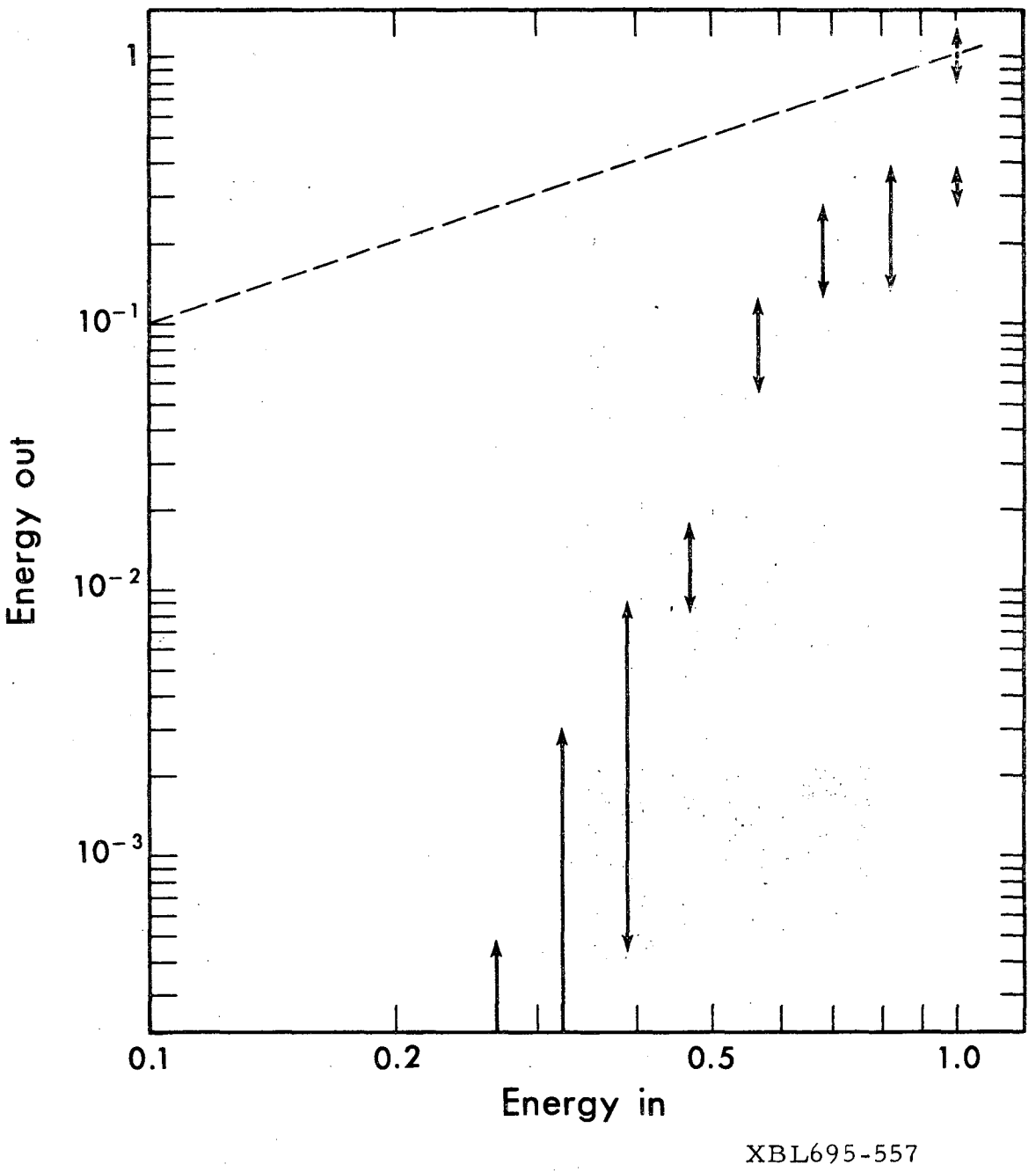


Fig. 13

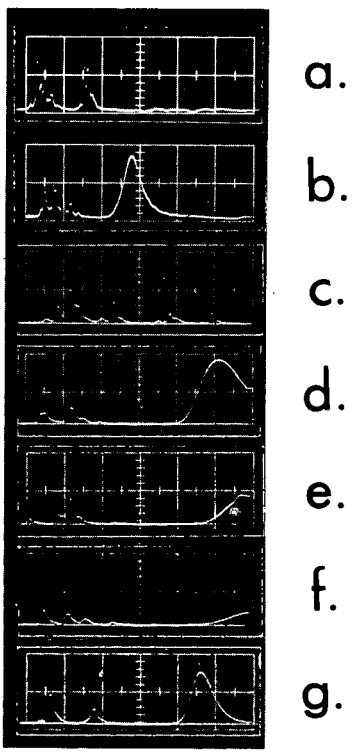


XBB 695-3385

Fig. 14

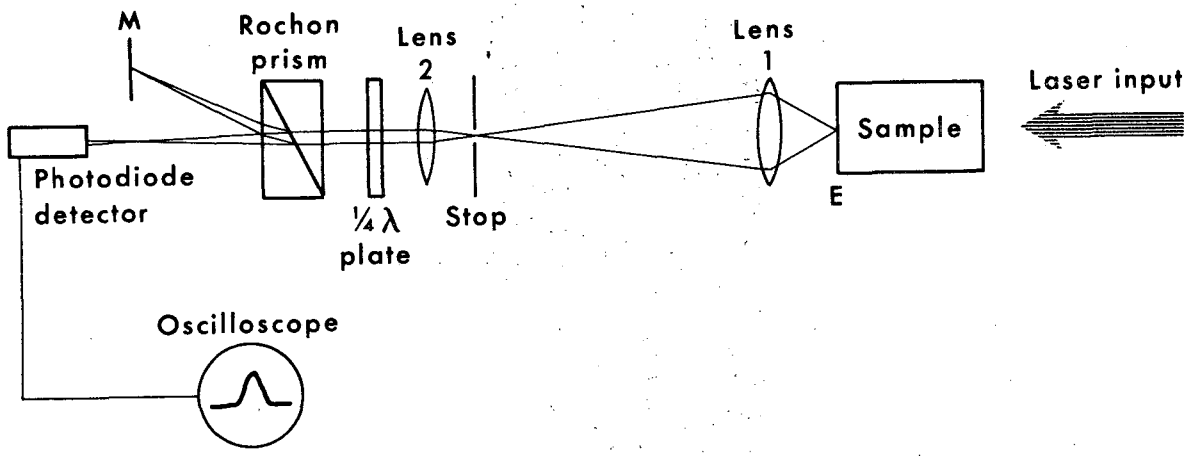


XBL695-558

Fig. 15

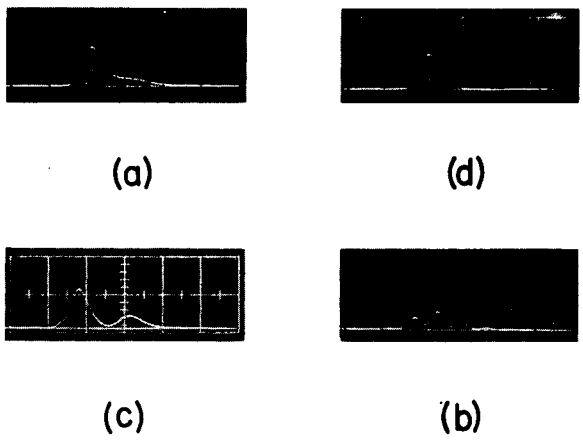


XBB 695-3386

Fig. 16

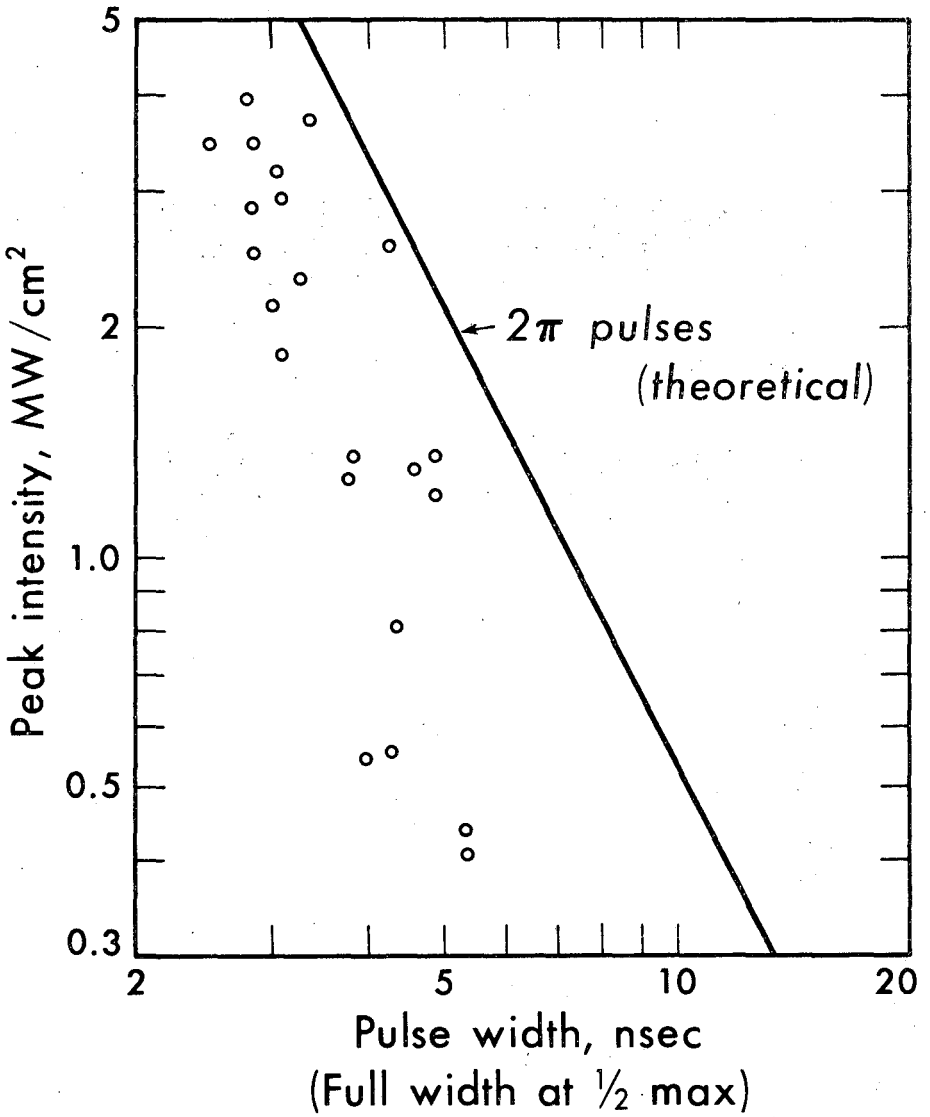


XBL695-559

Fig. 17

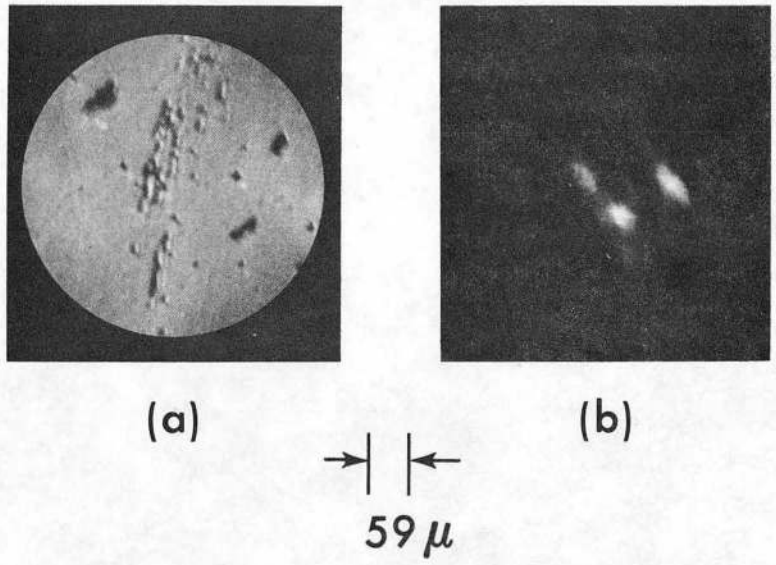


XBB 695-3387

Fig. 18

*TECHNICAL INFORMATION DIVISION*
*LAWRENCE RADIATION LABORATORY*
*UNIVERSITY OF CALIFORNIA*
*BERKELEY, CALIFORNIA 94720*